Chinese Herbal Medicines 13 (2021) 17–32

Contents lists available at ScienceDirect

Chinese Herbal Medicines

journal homepage: www.elsevier.com/locate/chmed

Original Article

An integrated strategy toward comprehensive characterization and quantification of multiple components from herbal medicine: An application study in *Gelsemium elegans*

Meng-ting Zuo [a,1], Yan-chun Liu [a,1], Zhi-liang Sun [a,b], Li Lin [a], Qi Tang [c], Pi Cheng [c], Zhao-ying Liu [a,b,c,*]

[a] College of Veterinary Medicine, Hunan Agricultural University, Changsha 410128, China
[b] Hunan Engineering Technology Research Center of Veterinary Drugs, Hunan Agricultural University, Changsha 410128, China
[c] Hunan Key Laboratory of Traditional Chinese Veterinary Medicine, Hunan Agricultural University, Changsha 410128, China

ARTICLE INFO

Article history:
Received 28 February 2020
Revised 11 June 2020
Accepted 16 June 2020
Available online 24 September 2020

Keywords:
Gelsemium elegans (Gardn. & Champ.) Benth
herbal medicine
LC-MS
mass spectrometry

ABSTRACT

Objective: To develop a powerful integrated strategy based on liquid chromatography coupled with mass spectrometry (LC-MS) systems for the comprehensive characterization and quantification of multiple components of herbal medicines.

Methods: Firstly, different mobile phase additives, analysis time, and MS acquisition modes were orthogonally tested with liquid chromatography coupled with quadrupole time-of-flight mass spectrometry (LC-QTOF/MS) in order to detect as many components of *Gelsemium elegans* as possible with high peak intensity. Secondly, several data mining strategies, including database searching, diagnostic ion filtering and neutral loss filtering, were utilized to perform chemical profiling. Subsequently, this study focused on the quantification and validation of the performance of a liquid chromatography-triple mass spectrometry (LC-QqQ/MS) assay based on derivative multiple reaction monitoring (DeMRM).

Results: A total of 147 components from *G. elegans* were characterized, among them 116 nontarget components were reported for the first time. A sensitive and reproducible LC-QqQ/MS method was successfully developed and validated for the simultaneous relative quantification of 41 components of *G. elegans*. This LC-QqQ/MS method was then applied to compare the contents of components in the roots, stems and leaves.

Conclusion: The present integrated strategy would significantly contribute to chemical studies on herbal medicine, and its utility could be extended to other research fields, such as metabolomics, quality control, and pharmacokinetics.

1. Introduction

There is rising global interest in herbal medicines as a promising source for new drug discovery and development (Shi et al., 2018; Wang, Shi, & Wang, 2018). The use of herbal medicines in the clinic also requires the elucidation of as many components as possible to ensure improved quality control and clinical outcomes. A significant feature of herbal medicine is the number of chemical components, as each herbal medicine contains hundreds or even thousands of different components, depending on the number of genes. These components are small molecules (<1500 Da) among many different chemical substance classes, which can be present in many different concentrations (Yan et al., 2013; Mustafa et al., 2018; Tan et al., 2018). Due to their high diversity, the comprehensive characterization and quantification of multiple components of herbal medicines remain a great challenge and bottleneck.

Currently, liquid chromatography coupled with various types of mass spectrometers, especially hybrid mass spectrometers, has been increasingly accepted as the predominant platform for the global analysis of complex herbal medicines. Among these mass spectrometry techniques, time-of-flight (TOF) mass spectrometry and liquid chromatography coupled with hybrid tandem mass spectrometry (LC-QTOF/MS) are expected to be the most powerful tools for structurally characterizing complex components of herbal medicines due to the high resolution of both precursor and product ions with these methods (Lei, Li, Cheng, Wang, & Meng, 2018; Zhang et al., 2017b; Zuo et al., 2018). Both types of information are important and reliable for identifying components. Previously,

* Corresponding author.
E-mail address: liu_zhaoying@hunau.edu.cn (Z.-y. Liu).
[1] These authors contributed equally to this work.

https://doi.org/10.1016/j.chmed.2020.06.002
1674-6384/

most reported methodologies have been limited to target components and mainly depended on the use of reference components and/or comparison with literature data (Huo, Du, Sun, Dong, & Wang, 2018; Li et al., 2015a). Considering that the reference components that can be obtained are limited and most components contained in herbal medicines are unknown (nontarget components), these methods are apparently insufficient for the comprehensive detection and characterization of the complicated components of herbal medicines.

The characterization of nontarget components of herbal medicines is never an easy task (Chingin, Makarov, Denisov, Rebrov, & Zubarev, 2014; Xue et al., 2016; Samanipour, Reid, Bæk, & Thomas, 2018). Great challenges remain in optimizing the detection of herbal medicines and processing and mining data from the complex information obtained. Recently, corresponding strategies based on diagnostic fragment ions, key ion filtering, and mass defect filtering have been developed to characterize nontarget components from complex mixtures (Hao et al., 2008; Cai et al., 2014; Zhang et al., 2016; Shi et al., 2017). However, it is worth noting that these studies mainly focused on qualitative aspects (Chen et al., 2016; Ma et al., 2016). Moreover, few studies on quantifying the amounts of multiple components or monitoring the chemical variations that are frequently present in different parts of herbal medicines during different seasons have been conducted due to the high diversity of components and lack of standards (Li et al., 2015b; Yang et al., 2013). Therefore, the development of more comprehensive and effective strategies for the simultaneous characterization of nontarget components and quantification of multiple components of herbal medicines in the absence of reference substances is imperative.

To address this challenge, the present study provides an integrated strategy to simultaneously identify target and nontarget components and monitors the concentrations of multiple components of herbal medicines. The general flowchart for this integral strategy is shown in Fig. 1. First, different mobile phase additives, analysis time and MS acquisition modes were orthogonally tested to detect as many components of herbal medicines as possible with high peak intensities based on LC-QTOF/MS. Then, various data mining techniques, including database searching, diagnostic ion filtering and neutral loss filtering, were used to characterize nontarget components under the optimized conditions. Furthermore, to determine the relative concentrations of the characterized components, we quantified and validated the performance of an LC-QqQ/MS method based on derivative multiple reaction monitoring (DeMRM). A single calibration curve was developed to calculate the relative contents of multiple components without authentic standards for each component.

The proposed strategy was demonstrated on the herbal medicine *Gelsemium elegans* (Gardn. & Champ.) Benth, a species of flowering plant in Loganiaceae family, is known as a toxic plant. In China, it is known as Gouwen, Dachayao or Duanchangcao (Ornduff, 1970) and has been used as a traditional Chinese medicine (TCM) for the treatment of rheumatoid arthritis, neuropathic pain, spasticity, skin ulcers and cancer for many years. The bioactive components of *G. elegans* have attracted much attention from chemists, pharmacologists and toxicologists in recent years due to their multiple biological effects, such as anti-inflammatory, immunomodulating, analgesic, anxiolytic, antitumor, and neuropathic pain-relieving properties (Ling et al., 2014; Liu et al., 2013; Meyer, Boujedaini, Patte-Mensah, & Mensah-Nyagan, 2013; Y. Xu et al., 2012a; Y.-K. Xu et al., 2012b; Zhang et al., 2015b). To date, a total of 121 alkaloids, 25 iridoids and a number of other components from a wide spectrum of secondary metabolite classes have been isolated from *G. elegans* and characterized (Jin et al., 2014; Liu et al., 2017b; Yamada, Kitajima, Kogure, Wongseripipatana, & Takayama, 2011; Zhang et al., 2017a).

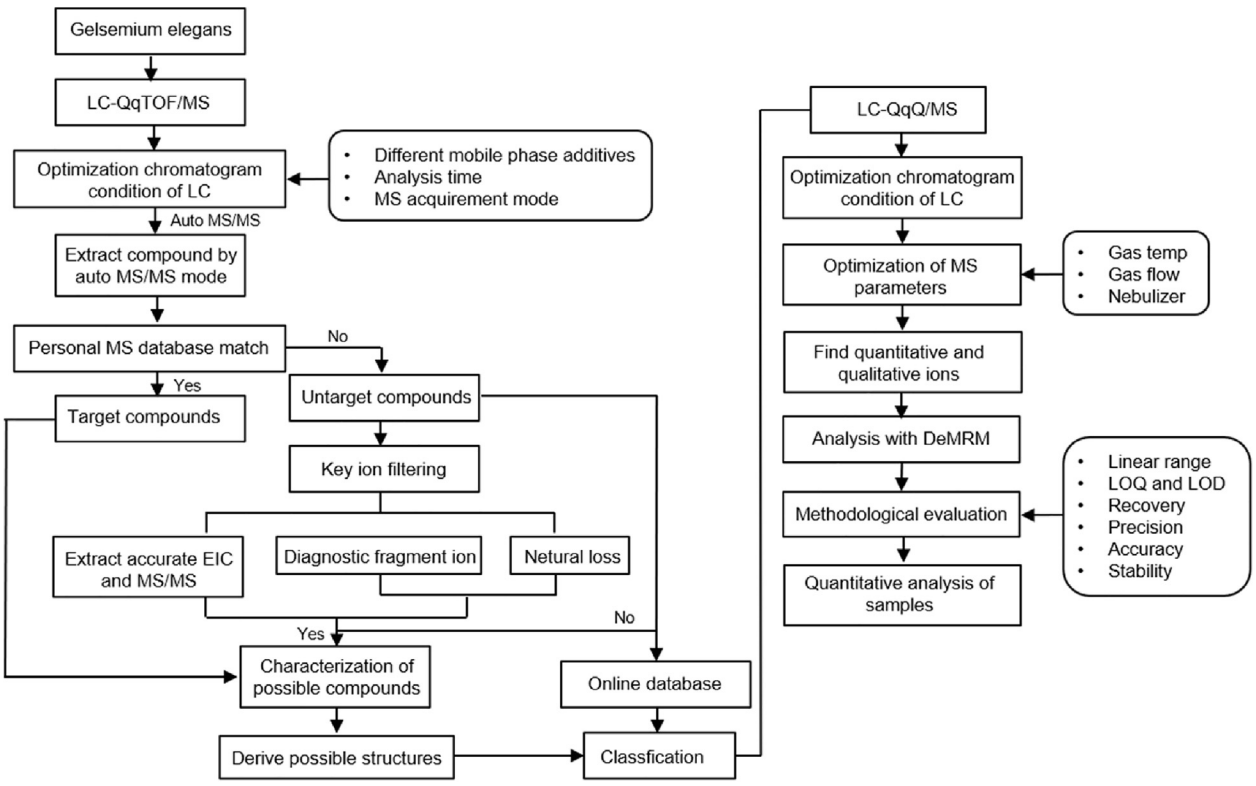

Fig. 1. Workflow of the integrated strategy toward comprehensive characterization of nontarget components and derivative multiple reaction monitoring for multiple components quantification of herbal medicine using LC-QTOF/MS and LC-QqQ/MS.

Previous studies have focused mainly on the isolation and purification of these components. Only our laboratory has recently published an analytical strategy for the characterization and structural analysis of target components from *G. elegans* by using LC-QTOF/MS based on the use of accurate mass databases combined with MS/MS spectra (Liu et al., 2017b; Xiao, Huang, Sun, & Liu, 2017; Yang et al., 2018a). However, many nontarget components in *G. elegans* have not been characterized. There are few reports on quantification methods for *G. elegans* formulations, and the number of analytes quantified in these reports is at most three (Hu et al., 2017; Liang et al., 2010; Wang, Wen, & Meng, 2018; Yang et al., 2018b; Zhang et al., 2015a). We developed a practical and reliable high-performance liquid chromatography-ultraviolet detector (HPLC-UV) method for fingerprint analysis using two major components, gelsemine and koumine. The results showed that at least seven relatively major components present in *G. elegans* may be useful for its quality control (Liu et al., 2017a). Using the methodology established in the study, a total of 147 components were characterized from *G. elegans*, and among these components, 116 nontarget components were reported for the first time. The simultaneous quantification of 41 components of *G. elegans* was achieved using DeMRM mode.

2. Materials and methods

2.1. Chemicals and materials

The reference components gelsemine (>98%), koumine (>98%), koumidine (>98%) and gelsenicine (>98%) were purchased from Shanghai Jiwei Biochemical Technology Co., Ltd. (Shanghai, China). HPLC-grade acetonitrile and methanol were purchased from Merck (Darmstadt, Germany). Ammonium formate, ammonium acetate, formic acid and acetic acid were purchased from SIGMA-ALDRICH (USA). Deionized water was purified by a Milli-Q water purification system (Bedford, MA, USA). The other chemicals used were of analytical grade. All reference components were weighed, dissolved in methanol and then diluted to appropriate concentrations for LC-QTOF/MS and LC-MS/MS analysis.

2.2. Plant materials and sample preparation

A total of nine samples including *G. elegans* roots, stems and leaves from three different periods were collected from Guangxi Province in China (see Supporting information, Table S1). The samples were authenticated by the author Qi Tang and stored at Hunan Key Laboratory of Traditional Chinese Veterinary Medicine. The samples were dried and then ground into powder. According to our optimized method, a 1 g aliquot of the powder was extracted twice by ultrasonication with 80% ethanol (1:25) for 0.5 h at 60 °C. The extraction solution was combined for filtration, and 1 mL of the filtered solution was evaporated and dissolved in 1 mL of acetonitrile-ammonium acetate (1:4, volume percent). Then, the solution was filtered through a 0.22 μm membrane before use. A 5 μL aliquot was injected for analysis.

2.3. LC-QTOF/MS conditions

Analysis was performed on an Agilent series 1290 Infinity HPLC instrument coupled with an Agilent 6530 Q-TOF mass spectrometer (Agilent Technologies, Santa Clara, CA, USA). Samples were separated on a Waters C_{18} column (3.5 μm, 4.6 mm × 150 mm). The flow rate was 0.3 mL/min, and the column temperature was maintained at 30 °C. To detect as many chemical components as possible with high peak intensities, an L9 (3) orthogonal array was used to examine the influence of difference mobile phase additives, gradient analysis times and MS acquisition mode (see Supporting information, Table S2). The gradient elution for 40 min was as follows: 0–2 min, 10% B; 2–7 min, 10% B to 15% B; 7–20 min, 15% B to 35% B; 20–30 min, 35% B to 90% B; 30–33 min, 90% B; 33.01–40 min, 10% B. The gradient elution for 50 min was as follows: 0–2 min, 10% B; 2–7 min, 10% B to 15% B; 7–30 min, 15% B to 45% B; 30–40 min, 45% B to 90% B; 40–43 min, 90% B; 43.01–50 min, 10% B. The gradient elution for 60 min was as follows: 0–2 min, 10% B; 2–7 min, 10% B to 15% B; 7–40 min, 15% B to 55% B; 40–50 min, 55% B to 90% B; 50–53 min, 90% B; 53.01–60 min, 10% B.

Mass spectrometric detection was performed in positive electrospray ionization (ESI) mode. The operating parameters were as follows: fragmentor voltage, 30 V; capillary voltage, 3500 V; dry gas temperature, 300 °C; sheath gas temperature, 350 °C; dry gas (N_2) flow rate, 9 L/min; sheath gas flow rate, 11 L/min; nebulizer, 35 psi; VCap, 4000; nozzle voltage, 1000 V; fragmentor, 175; Skimmer1, 65. Data were acquired in a mass range of m/z 50–1000. Auto MS/MS mode was utilized to obtain abundant structural information without knowledge of the sample. The collision energy (CE) was set at 10, 20, and 30 V.

The instrument performed internal mass calibration automatically using an automated calibrant delivery system. The calibration solution contained internal reference masses of m/z 121.0508 and 922.0098 in positive mode. All of the data acquisition was controlled by Agilent MassHunter workstation software (version B.01.03 Build 1.3.157.0 2).

2.4. LC-QqQ/MS and MS/MS conditions

Analysis was performed on an Agilent series 1290 Infinity HPLC instrument coupled with an Agilent 6460 QqQ/MS mass spectrometer (Agilent Technologies, Santa Clara, CA, USA). Samples were separated on a Waters C_{18} column (3.5 μm, 4.6 mm × 150 mm). The flow rate was 0.3 mL/min, and the column temperature was maintained at 30 °C.

Auto MS/MS analysis was performed in both scan mode and multiple reaction monitoring (MRM) mode. The MS/MS switching time and scan speed were set at < 2 ms and 5200 amu/s, respectively. The operating parameters were set as follows: scan range, m/z 50–1000; capillary temperature, 350 °C; capillary voltage, 3000 V; dry gas (N_2) flow rate, 12 L/min; nebulizer pressure, 40 psi. Full mass spectra were recorded at a mass resolving power of 0.7 Da (full width at half maximum).

2.5. Relative quantitation of multiple components

In the present study, DeMRM was used to obtain the mass responses of targeted analytes, and a koumidine calibration curve was employed instead of authentic standards to determine the concentrations of multiple components of *G. elegans*. The method was first validated with four representative components (gelsemine, koumine, koumidine and gelsenicine) in terms of linearity, limits of detection and quantification (LOD and LOQ), and intraday and interday precision. LOD and LOQ were determined at a signal-to-noise ratio of approximately 3 and 10, respectively. Intraday precision was determined by analyzing six replicates of each representative component at 10 ng/mL and 100 ng/mLl within one day, while interday precision was assessed on three consecutive days. Then, the DeMRM method was carried out with six *G. elegans* samples to demonstrate that the whole method was reliable and acceptable for multiple component quantification. Six samples were prepared separately according to the above method and analyzed to measure repeatability. To assess stability, the samples were exposed to ambient temperature and then analyzed at 0, 2,

4, 8, and 24 h. The relative concentrations of multiple components of *G. elegans* were calculated from the koumidine calibration curve.

3. Results and discussion

3.1. Optimization of LC-QTOF/MS conditions

This study examined different mobile phase additives, analysis times and MS acquisition modes, which could help to significantly improve the information obtained regarding the content of nontarget components in herbal medicines

The results of the detection of all components in *G. elegans* are shown in Fig. 2. These results showed that there were great differences in the number of *G. elegans* components detected under different test conditions. As shown in Fig. 2A, among the experimental groups, the number of components detected in the D and I groups was the smallest, and the number of components detected in the C and E groups was the highest. Relative to the number detected with the other two mobile phases, the total number of compounds detected in groups A, B and C with a 0.1% formic acid–water mobile phase was significantly large. The number of compounds detected in the corresponding groups C, F, and I with a consistent analysis time of 60 min was not significantly different from that detected in groups B, E, and H, corresponding to an analysis time of 50 min. As shown in Fig. 2A, the component peaks were mainly concentrated in the first 30 min of analysis, so the number of components did not change by extending the analysis time over 50 min. Fig. 2B showed that among the experimental groups, the peak intensities of the components in *G. elegans* in groups B, D, and I were the highest, and the intensities of the components in groups E and F were the lowest. These results suggested that compared to the other two acquisition modes, the auto MS/MS mode not only had higher peak intensities but also was more efficient. What's more, compared with ammonium acetate and ammonium formate as additives, an aqueous solution of 0.1% formic acid provided higher peak intensities. Thus, we recommend the application of a 50 min gradient, MS/MS mode and 0.1% formic acid to ensure better results.

3.2. Characterization of target components in G. elegans

The optimal LC-QTOF/MS conditions were used to acquire information about *G. elegans* sample No. S**1**. The first step of this analytical strategy was to extract components from raw acquisition data with the "Find by Auto MS/MS" function. The mass match tolerance was set to 0.05 *m*/*z*, and the peak abundance was set to 1000. Following this step, the target components were matched with personal database searching and characterized according to our published analytical approach (Liu et al., 2017b).

The precise mass of precursor ions (within ± 5 ppm) found to match data in the MS database of *Gelsemium* would give the exact element compositions and the possible known structure of the components. Structural characterization of the components was achieved on the basis of determining the accurate mass and fragmentation behavior of the product ions. A total of 31 components were matched with the personal database and characterized. Thirteen of them were gelsedine-type alkaloids, which was the largest class in *G. elegans*. They were components **28**, **40**, **75**, **83**, **94**, **100**, **109**, **110**, **118**, **124**, **126**, **131** and **134**. Components **99**, **117**, **119**, **128** and **143** were target sarpagine-type alkaloids obtained after matching. The $[M + H]^+$ ions of components **133** and **137** were *m*/*z* 355.2025 and 371.1974, respectively, which corresponded to humantenine-type alkaloids. Components **53** and **95** had masses of *m*/*z* 325.1917 and 307.1812, respectively, and were characterized as koumine-type alkaloids. Components **63** and **72** were target gelsemine-type alkaloids obtained after matching. Four kinds of iridoid components were detected by matching with *Gelsemium* database: **30**, **57**, **91** and **92**. Only two phenolic acids were detected in *G. elegans* after matching with the MS database.

3.3. Characterization of nontarget components in G. elegans

The second step was to characterize the nontarget components when a component fails to match the information in our personal database. Based on the fragmentation of the target components, common fragment ions and neutral loss ions could be classified into families. According to this idea, some post-acquisition data mining procedures, including key ion filtering, diagnostic ion filtering, neutral loss filtering and online database (Metlin and HMDB public database) searching, were performed in this study (Qiao et al., 2016). The structure of the nontarget components could be characterized by accurate MS/MS spectra and fragmentation comparisons. As a result, a total of 116 nontarget components were characterized. Table 1 summarized the exact mass, fragment ion, and retention time for the characterized components of *Gelsemium*

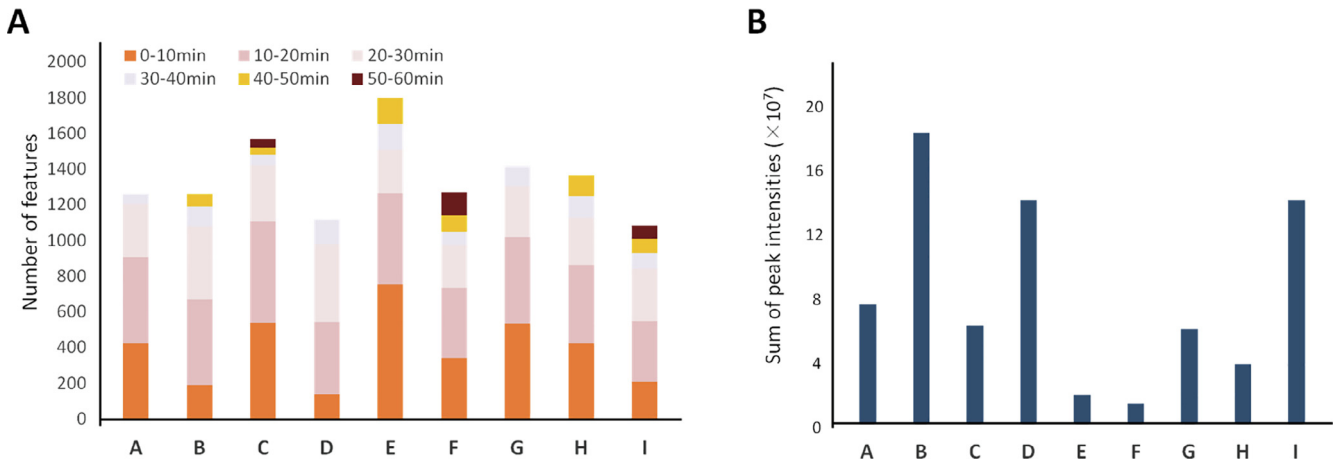

Fig. 2. Effect of mobile phases, analysis time and mass spectrometry modes on number of detected features (A) and sum of intensities (B) for *G. elegans* components. A, 0.1% FA, 40 min of gradient separation and MS mode; B, 0.1% FA, 50 min of gradient separation and auto MS/MS mode; C, 0.1% FA, 60 min of gradient separation and target MS/MS mode; D, 5 mmol/L NH_4Ac, 40 min of Gradient separation and auto MS/MS mode; E, 5 mmol/L NH_4Ac, 50 min of gradient separation and target MS/MS mode; F, 0.1% 5 mmol/L NH_4Ac, 60 min of Gradient separation and MS mode; G, 10 mmol/L NH_4F, 40 min of Gradient separation and target MS/MS mode; H, 10 mmol/L NH_4F, 50 min of gradient separation and MS mode; I, 10 mmol/L NH_4F, 60 min of gradient separation and auto MS/MS mode.

Table 1
Retention time, accurate mass, fragment ions of target and non-target compounds.

No.	t_R(min)	$[M+H]^+$	Fragment ions	Formula	Tentative characterization	Classification
1	5.4	150.0921	**132.0807**,117.0574,77.0383	$C_9H_{11}NO$	Unknown	Amino acid
2	5.5	521.2131	490.1948,**459.1777**,441.1624,403.1448,359.1604,328.1423,297.1249,279.1138,269.1286,256.0980,108.0806	$C_{25}H_{32}N_2O_{10}$	Unknown	Gelsedine-type
3	5.6	537.2074	506.1900,489.1864,**475.1775**,457.1617,375.1521,344.1369	$C_{25}H_{32}N_2O_{11}$	Unknown	Gelsedine-type
4	5.8	229.1551	170.0785,142.0858,132.0788,114.0550,96.0812,70.0659,58.0667	$C_{11}H_{20}N_2O_3$	Pro Leu or Pro Ile	Amino acid
5	6.0	236.1323	218.1163,150.0921,**132.0811**,117.0593,87.0449	$C_{13}H_{17}NO_3$	Unknown	Amino acid
6	6.4	195.0626	177.0483,149.0596,121.0621,91.0552,77.0366	$C_{10}H_{10}O_4$	Ferulic acid	Phenolic acids
7	6.4	213.0735	195.0627,177.0517,165.0518,**149.0568**,131.0466,121.0621,103.0519,**91.0523,**77.0370,69.0317,57.0323	$C_{10}H_{12}O_5$	Gelsemide	Iridoids
8	6.4	231.0841	216.1015,195.0604,177.0518,**149.0568**,121.0625,107.0465,93.0672,**91.0521**,77.0365,57.0321	$C_{10}H_{14}O_6$	Geleganoid A/GRIR-1	Iridoids
9	6.6	229.1536	195.0628,177.0517,142.0854,121.0626,70.0645	$C_{11}H_{20}N_2O_3$	Pro Leu or Pro Ile	Amino acid
10	6.8	199.0949	**135.0774**,121.0622,**117.0865**,109.0641,**91.0533**,79.0540,67.0542,55.0540	$C_{10}H_{14}O_4$	9-DeoxyGRIR-2	Iridoids
11	6.8	217.1057	163.0705,**135.0786**,109.0640,**91.0536**,79.0538,67.0535,55.0175	$C_{10}H_{16}O_5$	7-Hydroxygelsemiol/9-Hydroxygelsemiol	Iridoids
12	6.8	239.0877	177.0541	$C_{12}H_{14}O_5$	Hydroxyl of ferulic acid ethyl ester	Phenolic acids
13	7.0	408.1505	213.0748,195.0648,151.0738	$C_{17}H_{21}N_5O_7$	Unknown	Nucleoside
14	7.3	187.0959	109.0639,**105.0698**,95.0854,**91.0542**,81.0701,79.0544,77.0385,67.0553	$C_9H_{14}O_4$	7-Deoxygeleganoid D/9-Deoxygeleganoid D	Iridoids
15	7.7	217.1073	**135.0802**,117.0701,109.0650,**91.0540,**79.0549,67.0547,55.0186	$C_{10}H_{16}O_5$	Isomer of 7-Hydroxygelsemiol/9-Hydroxygelsemiol	Iridoids
16	7.8	239.0866	177.0534,84.0794,58.0655	$C_{12}H_{14}O_5$	Hydroxyl of ferulic acid ethyl ester	Phenolic acids
17	8.2	422.1295	325.0941,277.0637,213.0759,151.0761,133.0635	$C_{17}H_{19}N_5O_8$	Unknown	Nucleoside
18	8.3	236.1285	150.0906,**132.0791**,117.0553,87.0447	$C_{13}H_{17}NO_3$	Unknown	Amino acid
19	8.6	213.0759	195.0636,177.0543,**149.0583**,131.0477,121.0630,**91.0546,**77.0398,57.0344	$C_{10}H_{12}O_5$	Isomer of GEIR-1	Iridoids
20	8.8	187.0968	123.0804,**105.0708**,95.0855,**91.0564**,81.0691,77.0396,67.0550,55.0558	$C_9H_{14}O_4$	7-Deoxygeleganoid D /9-Deoxygeleganoid D	Iridoids
21	8.9	217.1059	**135.0848**,117.0683,**91.0559**,81.0576	$C_{10}H_{16}O_5$	Isomer of 7-Hydroxygelsemiol/9-Hydroxygelsemiol	Iridoids
22	8.9	407.1820	376.1611,345.1455,331.1300,166.0879	$C_{20}H_{26}N_2O_7$	Tihydroxygelsemicine	Gelsedine-type
23	9.2	422.1300	395.1598,213.0757,195.0638,175.0232,151.0750,129.0183,73.0295	$C_{17}H_{19}N_5O_8$	Unknown	Nucleoside
24	9.4	187.0966	123.0786,109.0650,**105.0707,**95.0852,**91.0536,**81.0698,77.0397,67.0548,55.0548	$C_9H_{14}O_4$	Isomer of 7-Deoxygeleganoid D /9-Deoxygeleganoid D	Iridoids
25	9.6	199.0937	**135.0776**,**117.0675**,115.0515,105.0667,**91.0521**,79.0522,67.0519,55.0162	$C_{10}H_{14}O_4$	9-Deoxygeleganoid F	Iridoids
26	9.6	217.1045	163.0717,**135.0781**,117.0676,109.0624,105.0669,**91.0521**,79.0525, 67.0526,55.0164	$C_{10}H_{16}O_5$	7-Hydroxygelsemiol/9-Hydroxygelsemiol	Iridoids
27	9.6	239.0855	177.0447,105.0674	$C_{12}H_{14}O_5$	Hydroxyl of ferulic acid ethyl ester	Phenolic acids
28	9.8	359.1578	328.1395,311.1366,**297.1212**,279.1105,269.1259,256.0960,228.0718,124.0740,108.0791,96.0790	$C_{19}H_{22}N_2O_5$	11,14-Dihydroxygelsenicine	Gelsedine-type
29	9.9	195.0642	177.0546,121.0623.91.0534,77.0375	$C_{10}H_{10}O_4$	Isomer of ferulic acid	Phenolic acids
30	9.9	213.0754	195.0644,177.0511,**149.0579**,121.0626,**91.0532**,79.0529,77.0372,57.0326,55.0171	$C_{10}H_{12}O_5$	GEIR-1	Iridoids
31	10.1	375.1553	344.1359,327.1335,**313.1175**,295.1072,279.1139,267.1137,124.0756	$C_{19}H_{22}N_2O_6$	11,14,15-Trihydroxygelsenicine	Gelsedine-type
32	10.7	187.0969	133.0695,123.0822,109.0638,**105.0706**,95.0847,**91.0544,**81.0702,79.0539,77.0386,67.0542,55.0541	$C_9H_{14}O_4$	Isomer of 7-Deoxygeleganoid D /9-Deoxygeleganoid D	Iridoids
33	10.7	417.1649	386.1485,**355.126**0,166.0854	$C_{21}H_{24}N_2O_7$	Isomer of 14-Acetoxy-dihydroxygelsenicine	Gelsedine-type
34	10.8	213.0738	177.0499,**149.0581,**121.0628,103.0522,**91.0529,**77.0374,67.0533,55.0532	$C_{10}H_{12}O_5$	Isomer of gelsemide	Iridoids
35	10.9	395.1603	364.1396,347.1355,**333.1212**,307.1060,277.0950,246.1106,228.0630,132.0789	$C_{22}H_{22}N_2O_5$	Unknown	Gelsedine-type
36	11.4	373.1768	342.1581,327.1357,**311.141**,271.1448,180.1024,122.0965,108.0810	$C_{20}H_{24}N_2O_5$	14,15-Dihydroxyrankinidine	Humantenine-type
37	11.5	339.1707	293.1616,236.1063,195.0677	$C_{20}H_{22}N_2O_3$	Gelsemine oxide	Gelsemine-type
38	11.6	408.1510	213.0765,195.0636,177.0518,167.0732,149.0606	$C_{17}H_{21}N_5O_7$	Unknown	Nucleoside
39	11.8	325.1913	307.1808,281.1644,238.1268,**220.1179**,194.0997,150.0908,130.06481,70.0655	$C_{20}H_{24}N_2O_2$	19-(*S*)-Hydroxydihydrokoumine/19-(*R*)-Hydroxydihydrokoumine	Coumine-type
40	11.9	329.1499	311.1387,**269.1300**,168.1021,148.0381,122.0949,108.0809	$C_{18}H_{20}N_2O_4$	Nb-Methylgelsedilam	Gelsedine-type
41	11.9	391.1869	360.1639,**329.1497**,311.1414,168.1018	$C_{20}H_{26}N_2O_6$	Dihydroxy gelsemicine	Gelsedine-type
42	12.2	361.1763	330.1564,**301.1184**,283.1101,162.0545,84.0812	$C_{19}H_{24}N_2O_5$	11,14-Dihydroxy-dihydrogelsenicine	Gelsedine-type
43	12.3	422.1293	213.0759,195.0642,177.0538,149.0578,121.0653	$C_{17}H_{19}N_5O_8$	Unknown	Nucleoside

(*continued on next page*)

Table 1 (*continued*)

No.	t_R(min)	$[M+H]^+$	Fragment ions	Formula	Tentative characterization	Classification
44	12.4	323.1757	293.1646,279.1496,198.0908,138.0907,70.0606	$C_{20}H_{22}N_2O_2$	Isomer of gelsemine	Gelsemine-type
45	12.4	377.1717	346.1527,**317.1131** ,299.1021,271.1068,232.1196,203.0812,138.0552	$C_{19}H_{24}N_2O_6$	11,14,15-Trihydroxy-dihydro gelsenicine	Gelsedine-type
46	12.7	339.1709	**323.1703**,252.1005,70.0657	$C_{20}H_{22}N_2O_3$	Gelsemine oxide	Gelsemine-type
47	12.9	311.1760	293.1654,252.1387	$C_{19}H_{22}N_2O_2$	Hydroxy of koumidine	Sarpagine-type
48	12.9	385.1769	354.1602,339.1356,**311.1336**,134.0956,122.0995	$C_{21}H_{24}N_2O_5$	15-Hydroxyhumantenox-enine	Humantenine-type
49	13.2	571.2292	540.2101,**509.1940**,481.1919,359.1604,328.1422,297.1245,	$C_{29}H_{34}N_2O_{10}$	Diydroxyl of gelseiridone/gelseganine D	Gelsedine-type
50	13.4	527.2389	508.2282,496.2177,479.2188,339.1347	$C_{28}H_{34}N_2O_8$	Unknown	Gelsedine-type
51	13.5	341.1866	**323.1742**,311.1156,297.1663,238.1224	$C_{20}H_{24}N_2O_3$	19S-Hydroxydihydrogelsemine	Gelsemine-type
52	13.5	391.1872	360.1683,**329.1499**,281.1284,238.0866,148.0396	$C_{20}H_{26}N_2O_6$	Dihydroxy gelsemicine	Gelsedine-type
53	13.7	325.1916	307.1810,281.1661,238.1226,**220.1116**,194.0995,70.0660	$C_{20}H_{24}N_2O_2$	19-(*S*)-Hydroxydihydrokoumine/19-(*R*)-Hydroxydihydrokoumine	Koumine-type
54	13.9	323.1750	307.1801,238.1236,**220.1118**,194.1006,150.0913,122.0960	$C_{20}H_{22}N_2O_2$	Koumine N-oxide	Koumine-type
55	14.1	422.1300	197.0816,179.0702,161.0589,153.0889,135.0796,108.0656	$C_{17}H_{19}N_5O_8$		Nucleoside
56	14.2	339.1712	325.1546,297.1603,252.1007,210.0910,70.0657	$C_{20}H_{22}N_2O_3$	Gelsemine oxide	Gelsemine-type
57	14.4	197.0817	**151.0752**,133.0639,115.0534,105.0703,**91.0547,**81.0705,79.0543,77.0383,67.0543	$C_{10}H_{12}O_4$	7-Deoxygelsemide /9-Deoxygelsemide	Iridoids
58	14.4	375.1558	344.1735,326.1625,**313.1450**,311.1388,299.1051,298.1672,122.0965,108.0809	$C_{19}H_{22}N_2O_6$	11,14,15-Trihydroxygelsenicine	Gelsedine-type
59	14.5	321.1604	291.1520,236.1068,210.0932,178.0846,136.0753	$C_{20}H_{20}N_2O_2$	Gelebolines A	Other types of alkaloids
60	14.7	327.1711	311.1756,297.1581,291.1470,238.1229,135.0806	$C_{19}H_{22}N_2O_3$	3-Hydroxykoumidine Oxide	Sarpagine-type
61	14.8	527.2396	509,2273,496.2207,479.2195,468.2315,339.1342	$C_{28}H_{34}N_2O_8$	Unknown	Gelsedine-type
62	14.9	355.1031	328.1448,309.1591,**163.0393,145.0286**,135.0442,117.0338,89.0400	$C_{16}H_{18}O_9$	1-*O*-Caffeoylquinic acid/4-*O*-Caffeoylquinic acid	Phenolic acids
63	15.1	341.1869	**323.1759**,311.1751,297.1605,281.1452,238.1221,158.0595,70.0656	$C_{20}H_{24}N_2O_3$	19R-Hydroxydihydrogelsemine	Gelsemine-type
64	15.2	197.0807	179.0702,**151.0745,**133.0646,115.0539,105.0697,**91.0544**,81.0699,79.0547,77.0385,67.0550	$C_{10}H_{12}O_4$	7-Deoxygelsemide /9-Deoxygelsemide	Iridoids
65	15.2	373.1759	342.1570,325.1550,**311.1394**,293.1285,108.0808	$C_{20}H_{24}N_2O_5$	11,14-Dihydroxyrankinidine	Humantenine-type
66	15.3	375.1919	357.1798,326.1625,**311.1388**,297.1584,283.1448,198.1100,122.0965,108.0809	$C_{20}H_{26}N_2O_5$	14,15-dihydroxy-19,20dihydrorankinidine	Humantenine-type
67	15.4	387.1913	369.1850,356.1697,341.1448,325.1548,**311.1734**,194.1165,138.0899	$C_{21}H_{26}N_2O_5$	Dihydrogelegamine A	Humantenine-type
68	15.5	394.1343	341.0486,295.0510,197.0804,179.0705,161.0593,153.0910,135.0804,108.0658	$C_{16}H_{19}N_5O_7$	Unknown	Nucleoside
69	15.6	343.1647	312.1465,295.1437,**281.1281**,264.1019,240.1012,212.0746,159.0673,108.080714,71.0734	$C_{19}H_{22}N_2O_4$	11-Hydroxygelsenicine	Gelsedine-type
70	15.6	505.2169	474.1980,**443.1818**,425.1636,339.1511,371.1530,341.0567,325.1311,297.1600,240.1194	$C_{25}H_{32}N_2O_9$	Unknown	Gelsedine-type
71	15.9	359.1606	328.1422,**285.1235**,95.0732	$C_{19}H_{22}N_2O_5$	Hydroxyl of gelseziridine	Gelsedine-type
72	16.2	323.1753	293.1627,262.1222,236.1072,70.0658	$C_{20}H_{22}N_2O_2$	Gelsemine	Gelsemine-type
73	16.2	424.1452	3397.0429,341.00501,197.0804,179.0698,161.0959,135.0805	$C_{17}H_{21}N_5O_8$	Unknown	Phenolic acids
74	16.7	359.1600	328.1420,311.1234,**297.1238**,279.1125,251.1168,225.1020	$C_{19}H_{22}N_2O_5$	14,15-Dihydroxygelsenicine	Gelsedine-type
75	16.8	343.1641	312.1473,**281.1289,**263.1181,253.1336,240.1033,212.0764,139.0990,124.0758,108.0811	$C_{19}H_{22}N_2O_4$	14-Hydroxygelsenicine	Gelsedine-type
76	17.0	406.1351	378.1419,343.1626,**197.0796**,179.0695,161.0591,153.0888,135.0792,107.0848,81.0729	$C_{17}H_{19}N_5O_7$	Unknown	Phenolic acids
77	17.2	339.1707	**323.1508,**312.1470,295.1451,281.1279,251.1339,108.0812	$C_{20}H_{22}N_2O_3$	Gelsemine N-oxide	Gelsemine-type
78	17.3	409.1756	378.1576,361.1555,**347.1380**,162.0904	$C_{23}H_{24}N_2O_5$	Unknown	Gelsedine-type
79	17.4	375.1911	344.1728,**313.1547**,295.1430,253.1331,168.1019	$C_{20}H_{26}N_2O_5$	11-Hydroxygelsemicine	Gelsedine-type
80	17.4	423.1558	392.1369,375.1340,**361.1186**,335.1069,305.0927,188.0714,176.0707,151.0633,107.0731	$C_{23}H_{22}N_2O_6$	Unknown	Gelsedine-type
81	17.6	379.1655	348.1469,331.1440,**317.1286**,291.1147,289.1335,261.1034,212.0706,132.0807,107.0734	$C_{22}H_{22}N_2O_4$	Unknown	Gelsedine-type
82	17.8	345.1818	314.1617,285.1230,267.1147,168.1011	$C_{19}H_{24}N_2O_4$	14-Hydroxygelsedine	Gelsedine-type
83	17.8	401.1712	370.1526,**339.1340**,311.1398,295.1131,166.0864,154.0849	$C_{21}H_{24}N_2O_6$	14-Acetoxy-15-hydroxygelsenicine	Gelsedine-type
84	17.9	361.1758	330.1571,**301.1181**,283.1078,271.1045,138.0544	$C_{19}H_{24}N_2O_5$	Isomer of 11,14-Dihydroxy-dihydro gelsenicine	Gelsedine-type
85	18.0	307.1802	293.1654,277.1697,251.1539,**220.1113**,138.0905,108.0806	$C_{20}H_{22}N_2O$	Isomer of koumine	Koumine-type
86	18.0	343.1651	312.1460,295.1495,**281.1281**,165.1330,108.0806,95.0730	$C_{19}H_{22}N_2O_4$	Hydroxyl of gelsenicine	Gelsedine-type

Table 1 (*continued*)

No.	t_R(min)	$[M + H]^+$	Fragment ions	Formula	Tentative characterization	Classification
87	18.0	449.1078	431.0937,413.0829,395.0740,377.0659,353.0643,329.0654,299.0547	$C_{21}H_{20}O_{11}$	Orientine/*iso*-orientine	Flavone
88	18.1	305.1653	277.1680,**220.1117**,162.0904,130.0650,120.0803,70.0655	$C_{20}H_{20}N_2O$	Dehydrokoumine	Koumine-type
89	18.2	311.1755	293.1656,269.1647,251.1546,**138.0918**,108.0816	$C_{19}H_{22}N_2O_2$	Hydroxy of koumidine	Sarpagine-type
90	18.2	428.2539	398.1746,339.0895,299.0594,118.0864	$C_{24}H_{33}N_3O_4$	Unknown	Oil
91	18.3	183.1009	**137.0908**,119.0842,107.0851,93.071,**91.0541**,77.0387,67.0545	$C_{10}H_{14}O_3$	GSIR-1	Iridoids
92	18.3	201.1118	147.0788,135.0788,**119.0845**,107.0843,93.0691,**91.0536**,81.0692,79.0538,77.0382, 67.0541,55.0180	$C_{10}H_{16}O_4$	Gelsemiol	Iridoids
93	18.3	369.1802	338.1611,**323.1733**,307.1432,178.1215,122.0952	$C_{21}H_{24}N_2O_4$	Gelsevirine N-oxide	Gelsemine-type
94	18.5	373.1767	342.1570,313.1564,**311.1394**,293.1285,283.1432,270.1129,189.0778,108.0808	$C_{20}H_{24}N_2O_5$	GS-2	Gelsedine-type
95	18.7	307.1810	277.1701,233.1229,**220.1122**,176.1074,130.0654,70.0658	$C_{20}H_{22}N_2O$	Koumine	Koumine-type
96	19.0	359.1611	328.1391,311.1351,**283.145**1,271.1076,254.0819,190.0723,150.0907,138.0909	$C_{19}H_{22}N_2O_5$	19,20-Dihydroxygelsenicine	Gelsedine-type
97	19.0	449.1084	413.0855,383.0752,353.0650,329.0650,299.0547,209.1642	$C_{21}H_{20}O_{11}$	Orientine/*iso*-orientine	Flavone
98	19.4	371.1966	340.1781,313.1542,**311.1404**,295.1437,277.1331	$C_{21}H_{26}N_2O_4$	15-hydroxyhumantenine	Humantenine-type
99	19.5	295.1802	277.1697,222.1269,156.0802,144.0806,**138.0908**,108.0807	$C_{19}H_{22}N_2O$	Koumidine	Sarpagine-type
100	19.5	375.1916	344.1723,**313.1540**,299.1388,265.1323,257.1268,198.1108,132.0441	$C_{20}H_{26}N_2O_5$	Hydroxylation of Gelsemicine	Gelsedine-type
101	19.6	359.1606	328.1405,311.1387,299.1414,281.0969,185.0702	$C_{19}H_{22}N_2O_5$	14,19-Dihydroxygelsenicine	Gelsedine-type
102	19.8	417.1655	386.1469,**368.1498**,341.1498,329.1128,323.13838,311.1122,283.1073,194.0804	$C_{21}H_{24}N_2O_7$	14-Acetoxy-dihydroxygelsenicine	Gelsedine-type
103	19.9	391.1868	360.1680,331.1283,**329.1478**,313.1176,217.0959,138.0546	$C_{20}H_{26}N_2O_6$	Dihydroxy gelsemicine	Gelsedine-type
104	20.1	369.1816	325.1542,**311.1405**,295.1418	$C_{21}H_{24}N_2O_4$	Humantenoxenine	Humantenine-type
105	20.2	433.1975	402.1784,**371.1601**,343.1628,311.1386,283.1443,150.0915	$C_{22}H_{28}N_2O_7$	11-Hydroxy-14-acetoxygelselegine	Gelsedine-type
106	20.3	371.1977	340.1774,325.1548,**323.1762**,138.0913	$C_{21}H_{26}N_2O_4$	19(*R*)-Hydroxydihydrogelsevirine/19(*S*)-hydroxydihydrogelsevirine	Gelsemine-type
107	20.9	371.1973	340.1772,**323.1750**,212.0715,122.0961	$C_{21}H_{26}N_2O_4$	19(*R*)-Hydroxydihydrogelsevirine/19(*S*)-hydroxydihydrogelsevirine	Gelsemine-type
108	21.1	295.1816	277.1700,247.1239,156.0806,144.0812,**138.0918**,120.0813,108.0814	$C_{19}H_{22}N_2O$	Isomer of koumidine	Sarpagine-type
109	21.1	405.2028	374.1823,**343.1652**,329.1502,325.1525	$C_{21}H_{28}N_2O_6$	11-Methoxy-19-(*R*)-hydroxygelselegine	Gelsedine-type
110	21.3	327.1720	296.1534,**265.1357**,225.1055,108.0825,95.0747,71.0750	$C_{19}H_{22}N_2O_3$	Gelsenicine	Gelsedine-type
111	21.6	371.1966	340.1782,325.1552,**311.1410**,178.1229,122.0965	$C_{21}H_{26}N_2O_4$	6-hydroxyhumantenine	Humantenine-type
112	21.9	357.1809	326.1632,**311.1397**,297.1263,269.1285,178.1228,164.1073,122.0967,108.0816	$C_{20}H_{24}N_2O_4$	14-Hydroxyrankinidine	Humantenine-type
113	22.1	353.1865	**323.1722**,322.1675,291.1491,164.1067,108.0809	$C_{21}H_{24}N_2O_3$	Gelsevirine	Gelsemine-type
114	22.5	343.1663	312.1480,**281.1265**,255.1127,238.0867,210.0915,174.0783,136.0785,118.0653	$C_{19}H_{22}N_2O_4$	Hydroxyl of gelsenicine	Gelsedine-type
115	22.6	325.1914	307.1796,281.1658,243,1500,158.0617,136.1124	$C_{21}H_{26}N_2O_2$	Gardnerine	Sarpagine-type
116	22.8	363.1712	332.1515,**301.1133**,261.1032,212.0702,144.0803,121.0855	$C_{22}H_{22}N_2O_3$	Unknown	Gelsedine-type
117	22.9	311.1761	293.1674,267.1490,249.1398,229.1338,158.0605,**138.0900**,122.0964,108.0815	$C_{19}H_{22}N_2O_2$	3-Hydroxykoumidine	Sarpagine-type
118	22.9	357.1811	326.1625,297.1428,**295.1442**,278.1185,254.1174,213.0919,108.0813,71.0740	$C_{20}H_{24}N_2O_4$	4,20-Dehydrogelsemicine	Gelsedine-type
119	22.9	383.1970	365.1857,341.1872,321.1592,180.1017,172.0753,**138.0913**	$C_{22}H_{26}N_2O_4$	Gelsempervine A	Sarpagine-type
120	23.7	339.1709	308.1521,277.1339,225.1019,176.1067,148.1119,114.0918	$C_{21}H_{26}N_2O_2$	Nb-Demethylgelsevirine	Gelsemine-type
121	23.7	533.2496	515.2388,502.2278,484.2206,467.2177,**453.2030**,381.1824,353.1859,339.1698	$C_{27}H_{36}N_2O_9$	Unknown	Gelsedine-type
122	23.9	309.1963	291.1840,265.1713,**220.1113**,178.1226,122.0960	$C_{20}H_{24}N_2O$	Dihydrokoumine	Koumine-type
123	23.9	353.1870	322.1677,295.1721,291.1488,239.1178,121.0883	$C_{21}H_{24}N_2O_3$	19-(*Z*)-Akuammidine	Sarpagine-type
124	23.9	359.1964	328.1778,**297.1602**,279.1484,222.0943,182.1161	$C_{20}H_{26}N_2O_4$	Gelsemicine	Gelsedine-type
125	23.9	417.2016	399.1909,376.1818,368.1717,357.1786,326.1627,298.1686,269.1284,163.0985	$C_{22}H_{28}N_2O_6$	Unknown	Gelsedine-type
126	24.1	385.1764	354.1573,**323.1407**,311.1390,295.1444,263.1179,237.1045,121.0880,108.0812,95.0732	$C_{21}H_{24}N_2O_5$	14-Acetoxygelsenicine	Gelsedine-type
127	24.3	517.1342	488.1965,443.1667,163.0386,145.0282,117.0338	$C_{25}H_{24}O_{12}$	1,3-dicaffeoylquinic acid	Phenolic acids
128	24.9	369.1812	323.1412,309.1539,307.1439,265.1079,172.1063,148.1113,122.0964,107.0742	$C_{21}H_{24}N_2O_4$	19*E*-16-epi-Voacarpine	Sarpagine-type
129	25.0	329.1859	298.1671,**269.1279**,257.1167,152.1059,84.0808	$C_{19}H_{22}N_2O_3$	Gelsedine	Gelsedine-type
130	25.1	417.2016	386.1832,**355.1651**,343.1652,295.1433,225.1015,150.0907	$C_{22}H_{28}N_2O_6$	14-Acetoxygelselegine	Gelsedine-type
131	25.5	389.2069	358.1881,**327.1703**,309.1577,284.1405	$C_{21}H_{28}N_2O_5$	11-Methoxygelselegine	Gelsedine-type

(*continued on next page*)

Table 1 (*continued*)

No.	t_R(min)	$[M+H]^+$	Fragment ions	Formula	Tentative characterization	Classification
132	25.7	357.2166	326.1984,**311.1773**,298.2032,239.1178,181.1452,124.1115	$C_{21}H_{28}N_2O_3$	19,20-Dihydrohumantenine	Humantenine-type
133	25.9	355.204	325.1911,324.18556,**311.1703**,310.1658,309.1625,178.1253122.0992	$C_{21}H_{26}N_2O_3$	Humantenine	Humantenine-type
134	25.9	429.2018	398.1839,385.1536,353.1862,**339.1695**,222.1110,166.0849,122.0946	$C_{23}H_{28}N_2O_6$	Gelseoxazolidinine	Gelsedine-type
135	26.1	309.1616	295.1466,281.1322,**138.0939**,132.0478,120.0813,108.0847	$C_{19}H_{20}N_2O_2$	Oxokoumidine	Sarpagine-type
136	26.1	341.1896	**311.1749**,310.1712,295.1483,281.1355,178.1266,164.1109,122.1003,108.0850,96.0849	$C_{20}H_{24}N_2O_3$	Rankinidine (Gelsemamides)	Humantenine-type
137	27.4	371.1951	340.1764,325.1531,**311.1396**,164.1055,122.0946,108.0797	$C_{21}H_{26}N_2O_4$	11-hydroxyhumantenine	Humantenine-type
138	27.5	385.2134	354.1920,339.1716,**311.1720**,178.1228,122.0972	$C_{22}H_{28}N_2O_4$	11-Methoxyhumantenine	Humantenine-type
139	27.8	357.2162	326.1968,**311.1726**,297.1587,181.1431,124.1223	$C_{21}H_{28}N_2O_3$	Isomer of 19,20-Dihydrohumantenine	Humantenine-type
140	28.9	373.2127	342.1929,327.1680,**313.1549**	$C_{21}H_{28}N_2O_4$	Acetyl of 14-Hydroxygelsedine	Gelsedine-type
141	29.7	325.1911	294.1728, 279.1519, 164.1066	$C_{20}H_{22}N_2O_2$	Na-Desmethoxyhumante-nine	Humantenine-type
142	30.2	273.1388	257.1064,254.1068	$C_{19}H_{16}N_2$	Sempervirine	Yohimbane
143	30.6	339.2068	308.1862,293.1644,279.1541,178.1221,164.1068,148.1117,136.1116,122.0961,108.0815	$C_{21}H_{26}N_2O_2$	Na-Methoxy-19(Z)anhydrovobasinediol	Sarpagine-type
144	33.6	343.1654	312.1450,281.1317,265.1067,255.1137,238.0862,210.0917,174.0872,118.0860	$C_{19}H_{22}N_2O_4$	Hydroxyl of gelsenicine	Gelsedine-type
145	36.0	343.1655	312.1448,295.1285,281.1294,265.1071,255.1113,238.0862,210.0991,174.0773,136.0750	$C_{19}H_{22}N_2O_4$	Hydroxyl of gelsenicine	Gelsedine-type
146	40.0	343.1184	327.0868,313.0706,299.0907,282.0881	$C_{19}H_{18}O_6$	Unknown	Flavone
147	40.7	279.1598	265.0186,219.1034,149.0232,121.0285,93.0342,57.0706	$C_{16}H_{22}O_4$	Phthalic acid dibutyl ester	Oil

elegans. They could be divided into seven groups according to their structural types and MS/MS fragmentation pathways.

3.3.1. Characterization of gelsedine-type alkaloids

A total of 52 components were recognized as gelsedine-type alkaloids. Based on the fragmentation behavior of these components, they contained a N_a-methoxy group. On the one hand, there was also a methoxy group on the C-11 position for some components; on the other hand, some of the components had a CH_2OH group at this position. Therefore, the main fragmentation pattern of components could be a neutral loss of 62 Da (two OCH_3 or OCH_3 plus CH_2OH). The neutral loss chromatogram (pNLC) of *m*/*z* 62 was shown in Fig. 3. For example, components **74** and **124** displayed $[M+H]^+$ ions at *m*/*z* 359.1600 and 359.1964, respectively. Both of them showed a fragment loss of 62 Da. However, for component **74**, a fragment of *m*/*z* 279 (M + H-80 Da) was lost, indicating that component **74** had more than one hydroxyl group; moreover, component **74** was an isomer of **28**. Therefore, components **74** and **124** were characterized as 14,15-dihydroxygelsenicine and gelsemicine, respectively.

The fragment ions of component 58 were *m*/*z* 344, 327, and 267, which were each 16 Da higher than the corresponding fragment ions *m*/*z* 328, 311, and 251 of component **96**, respectively. Therefore, component **58** was the hydroxylated product of component **96**. Components **58** and **45** provided the same fragment ion at *m*/*z* 299 by loss of a C_2H_3 or C_2H_5 group, respectively, indicating that component **45** was a reduction product of component **58**. Components **41** and **52** were 16 Da and 32 Da higher in molecular mass than components **100** and **124**, respectively, suggesting that they were dihydroxylation products of gelsemicine. The fragmentation pathways of the gelsedine-type alkaloids were summarized in Fig. 4.

3.3.2. Characterization of sarpagine-type alkaloids

Compared with the target components, component **99** was characterized as koumidine. Furthermore, component **108** was an isomer of **99**. According to the fragmentation pathway of koumidine (**99**), component **117** was characterized as a hydroxylated derivative of component **99**. Components **89** and **117** were characterized as 3-hydroxykoumidine and hydroxylated koumidine, respectively. Component **60** was the N-oxide form of 3-hydroxykoumidine. The sarpagine-type components could first lose the group at the N_a position, C-3 position or C-16 position. The diagnostic ion of these alkaloids was *m*/*z* 138. Components **123** and **113** had the same molecular formula, but component **113** had a diagnostic ion at *m*/*z* 323. The most abundant fragment ion of component **123** was at *m*/*z* 295. Therefore, component **123** was characterized as 19-(*Z*)-akuammidine. The fragmentation pathway of the sarpagine-type alkaloids was shown in Fig. 5.

3.3.3. Characterization of humantenine-type alkaloids

The key filter ions of humantenine-type alkaloids were *m*/*z* 311.17 (components **67**, **132**, **133**, **136**, **138** and **139**) and 311.14 (components **36**, **48**, **65**, **66**, **98**, **104**, **111**, **112** and **137**). The results indicated that humantenine-type alkaloid components could be found by filtering *m*/*z* 311 in the extracted-ion chromatogram (EIC) MS/MS spectrum. The EIC MS/MS spectrum of *m*/*z* 311 was shown in Fig. 6. These components could lose H_2O, hydroxymethyl, methoxy, methyl, or methylene groups to form the fragment ion at *m*/*z* 311. For example, component **112** could lose OCH_3 and CH_3 groups to form *m*/*z* 311, and component **137** could lose CH_2 after losing 46 Da (OCH_3 plus CH_3) to form *m*/*z* 311. The molecular formulas of compounds **98**, **111**, and **137** were calculated as $C_{21}H_{26}N_2O_4$ based on their measured accurate mass of *m*/*z* 371.196, which suggested that components **98**, **111**, and **137** were isomers. Components **36** and **65** were 16 Da higher in molecular weight than component **112**, which showed they were formed by

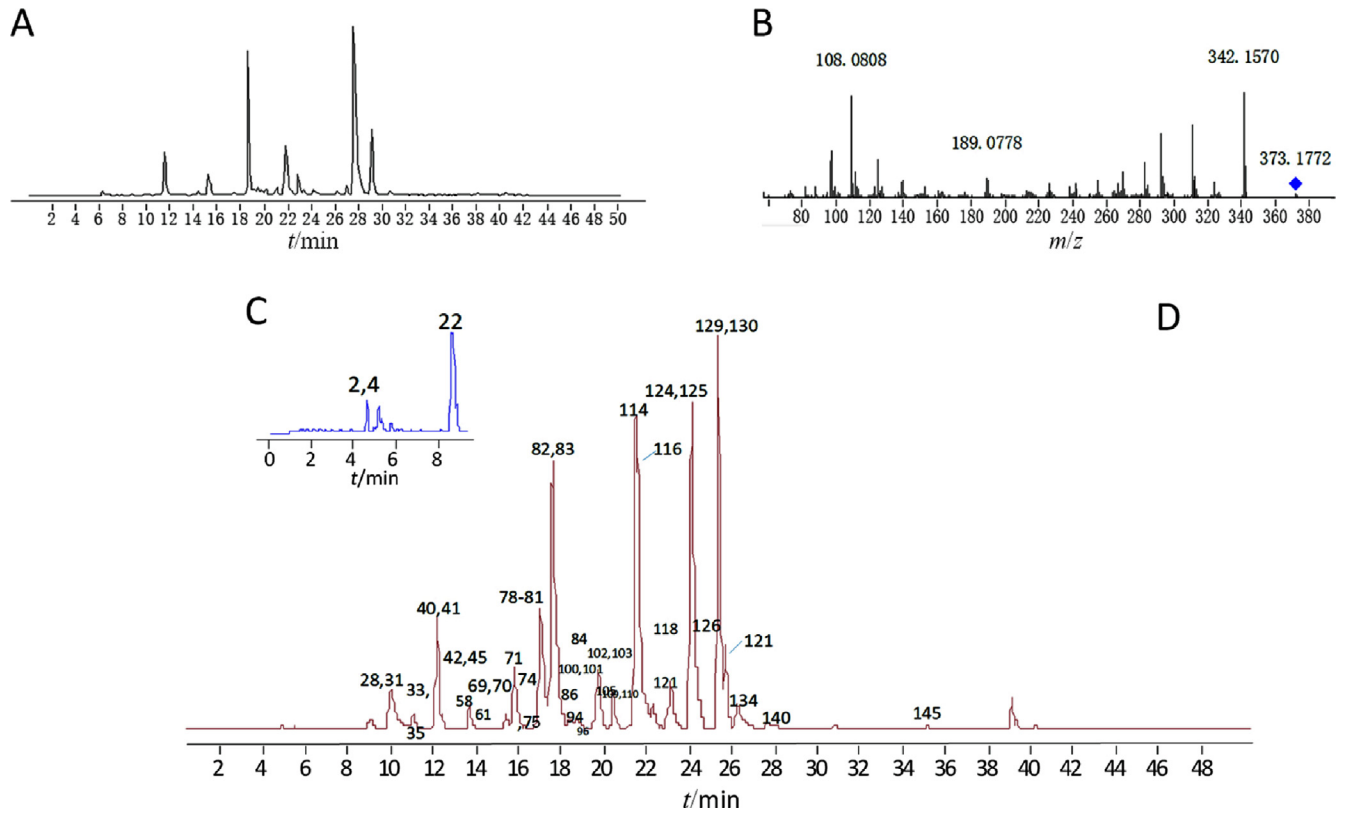

Fig. 3. EIC spectrum (A), MS/MS spectrum (B) of component **94** (GS-2), pNLC spectrum of gelsedine type alkaloids with neutral loss ion at *m*/*z* 62 (C) and pNLC spectrum of *G. elegans* compounds (D).

dihydroxylation of component **112**. As a result, components **112** and **137** were characterized as 14-hydroxyrankinidine and 11-hydroxyhumantenine, respectively. Through online database searching, component **104** was tentatively characterized as humantenoxenine, which belonged to the humantenine-type alkaloid family. The fragmentation pathways of the humantenine-type alkaloids were shown in Fig. 6.

3.3.4. Characterization of gelsemine-type alkaloids

The precursor ions of 11 gelsemine-type alkaloids, including compounds **46**, **44**, **51**, **56**, **63**, **72**, **77**, **93**, **106**, **107**, and **113** were screened out by using the diagnostic ion at *m*/*z* 323. The fragmentation pathways of the gelsemine-type alkaloids were shown in Fig. S1. These components would first lose the group at the N_a position, the methyl at the N_b position and the group at the C-19 position to form the diagnostic ion at *m*/*z* 323. For example, components **106** and **107** could lose OCH_3 (31 Da) to form the product ion at *m*/*z* 340 and then could lose OH (17 Da) at the C-19 position to form *m*/*z* 323. Based on the fragmentation data and accurate mass values, components **106** and **107** were a pair of isomers and were characterized as 19(*R*)-hydroxydihydrogelsevirine or 19(*S*)-hydroxydihydrogelsevirine, respectively. Component **120** was 14 Da lower in molecular weight than component **113** (loss of a methyl group at the N_b position), and component **93** was 16 Da higher in molecular weight than component **113** (N_b position). Thus, components **120**, **113**, and **93** were characterized as N_b-demethylgelsevirine, gelsevirine and gelsevirine N-oxide. Furthermore, components **37**, **46**, **56**, and **77** were the oxidized form of components **44** or **72**.

3.3.5. Characterization of koumine- type alkaloids

A total of seven components, compounds **39**, **53**, **54**, **85**, **88**, **95**, and **122** were classified as koumine-type alkaloids since they all yielded a diagnostic ion at *m*/*z* 220. Koumine-type alkaloids could gradually lose the groups at the C-19 position, N_b position, C-16 and C17 positions. The fragmentation pathways of the koumine-type alkaloids are shown in Fig. S2. By comparison to a koumine standard, component **95** was characterized as koumine. Component **95** was 2 Da higher in molecular weight than component **88**, and components **95** and **88** had the same fragment ions, which showed that component **88** was the dehydrogenation product of component **95**. Therefore, component **88** was named dehydrokoumine. Components **39** and **53** also had the same fragment ions and were characterized as 19-(*S*)-hydroxydihydrokoumine and 19-(*R*)-hydroxydihydrokoumine by literature searching (Kitajima, Kobayashi, Kogure, & Takayama, 2010), respectively.

3.3.6. Characterization of iridoids

Iridoids were filtered by a neutral loss of 46 Da (CH_2O_2) and a diagnostic ion at *m*/*z* 91. This filtering could be applied to EIC MS/MS and pNLC spectra due to the structure of iridoids. For example, components **10** and **25** had the same formula, but component **25** could lose 82 Da ($2H_2O$ plus CH_2O_2), whereas component **10** could lose only 64 Da (H_2O plus CH_2O_2), which proved that compared to component **10**, component **25** had an additional hydroxyl group. Components **11** and **26** were 16 Da higher in molecular weight than component **92** and were characterized as 7-hydroxygelsemiol or 9-hydroxygelsemiol, respectively. Through the combination of target ion and database searching, the nontargeted components were characterized quickly. The fragmentation pathways of the iridoids are shown in Fig. S3.

3.3.7. Characterization of phenolic acids

Only two types of phenolic acids were detected in *G. elegans* after matching with the MS database, and their structures were determined based on the MS/MS spectra. Component **62** produced

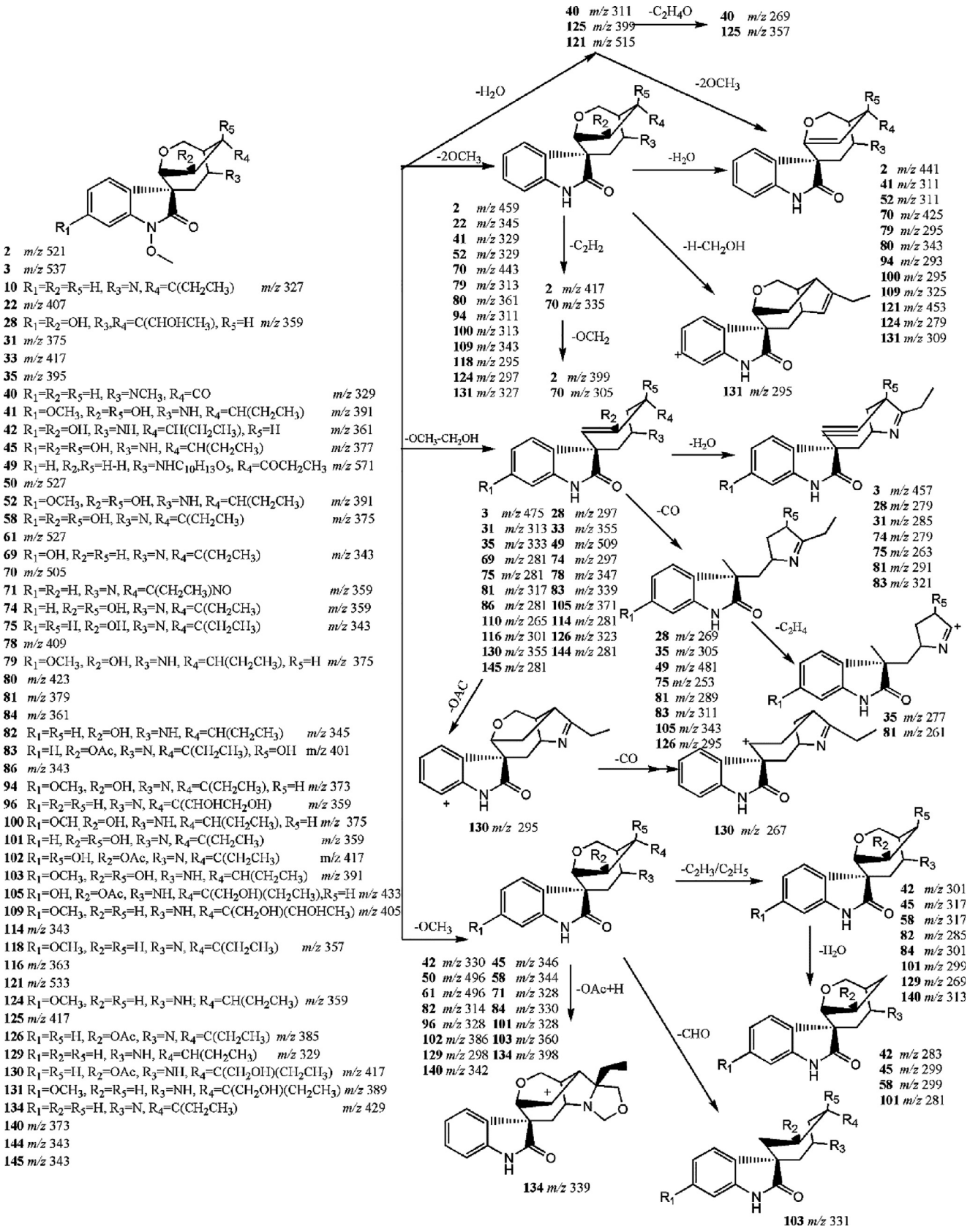

Fig. 4. Mass spectral fragmentation pathways of gelsedine-type alkaloids.

a sodium-adduct molecular ion $[M + Na]^+$ at *m*/*z* 377.0866 and a protonated molecular ion $[M + H]^+$ at 355.1024, and the enriched fragment ion at *m*/*z* 163 formed by losing glucuronic acid from the protonated molecule. The ion at *m*/*z* 145.0291 was formed by the loss of a molecule of H_2O (18 Da) from *m*/*z* 163.0394. The minimum ion at *m*/*z* 89.0403 was generated by the neutral loss of two

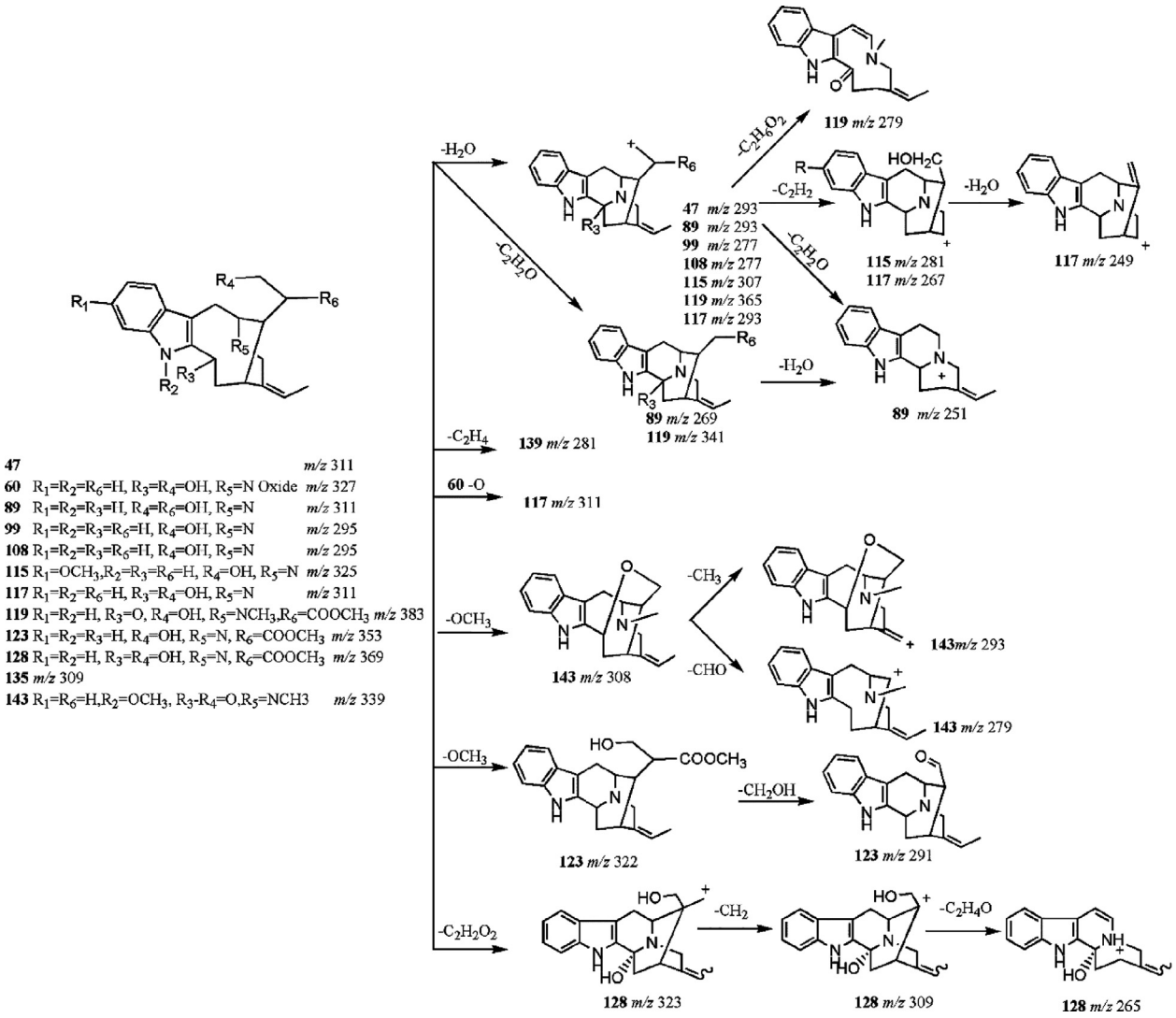

Fig. 5. Mass spectral fragmentation pathways of sapargine-type alkaloids.

CO molecules (28 Da) at *m/z* 145.0291. The structure of the phenolic acids was based on a benzene ring and numerous hydroxyl groups, so its fragment ions were formed by losses of H_2O and CO. Component **6** was established as ferulic acid, and it was proposed as an isomer of component **29**. Component **62** was characterized tentatively as 1-*O*-caffeoylquinic acid or 4-*O*-caffeoylquinic acid. Through an online database search, components **12**, **16**, **27**, **73**, and **127** were classified as phenolic acids. In addition, components **12**, **16**, and **27** were hydroxylated derivatives of ethyl ferulic acid.

3.4. MRM transitions derived from MS^2

With a combination of LC-QTOF/MS and LC-QqQ/MS, we developed a quantitative approach for analysis in the absence of standards. The present LC-MS/MS strategy enabled the separation of 41 components in the method validation protocol. Many parameters must be optimized during the development of a DeMRM method, which is always laborious and time-consuming. Therefore, a simple standard operation procedure was recommended in the present study.

First, the precursor ions and corresponding product ions of each component were obtained by LC-QTOF/MS and were used to form an ion pair; in general, each precursor ion had 2–3 product ions. Second, higher precursor ion and product ion responses were obtained through adequate optimization of instrumental parameters by repeatedly testing four standards (gelsemine, koumine, koumidine and gelsenicine) in reference multiple reaction monitoring (RMRM) mode. Finally, multiple components of *G. elegans* were optimized in terms of ion pairs and CE in LC-QqQ/MS (Table 2).

To avoid interference with some low-concentration components, ion pairs were set to several segments to improve sensitivity. The multiple components need to be optimized in terms of the analysis time period by adjusting the LC conditions to ensure good peak shape without tailing and drift. In addition, it is observed that compounds with similar structures are often assigned similar MRM parameters and transitions. Therefore, we developed a DeMRM method to monitor multiple components in herbal medicines, even those present at a trace level. In this study, *G. elegans* was selected as an example to demonstrate our approach. The retention times, monitored ion pairs, and related voltage parameters of multiple components in *G. elegans* were shown in Table 2.

3.5. Method validation of proposed method

Table S3 summarized the validation results of the four representative components (gelsemine, koumine, koumidine and gelsenicine) for RMRM. The correlation coefficients of the four

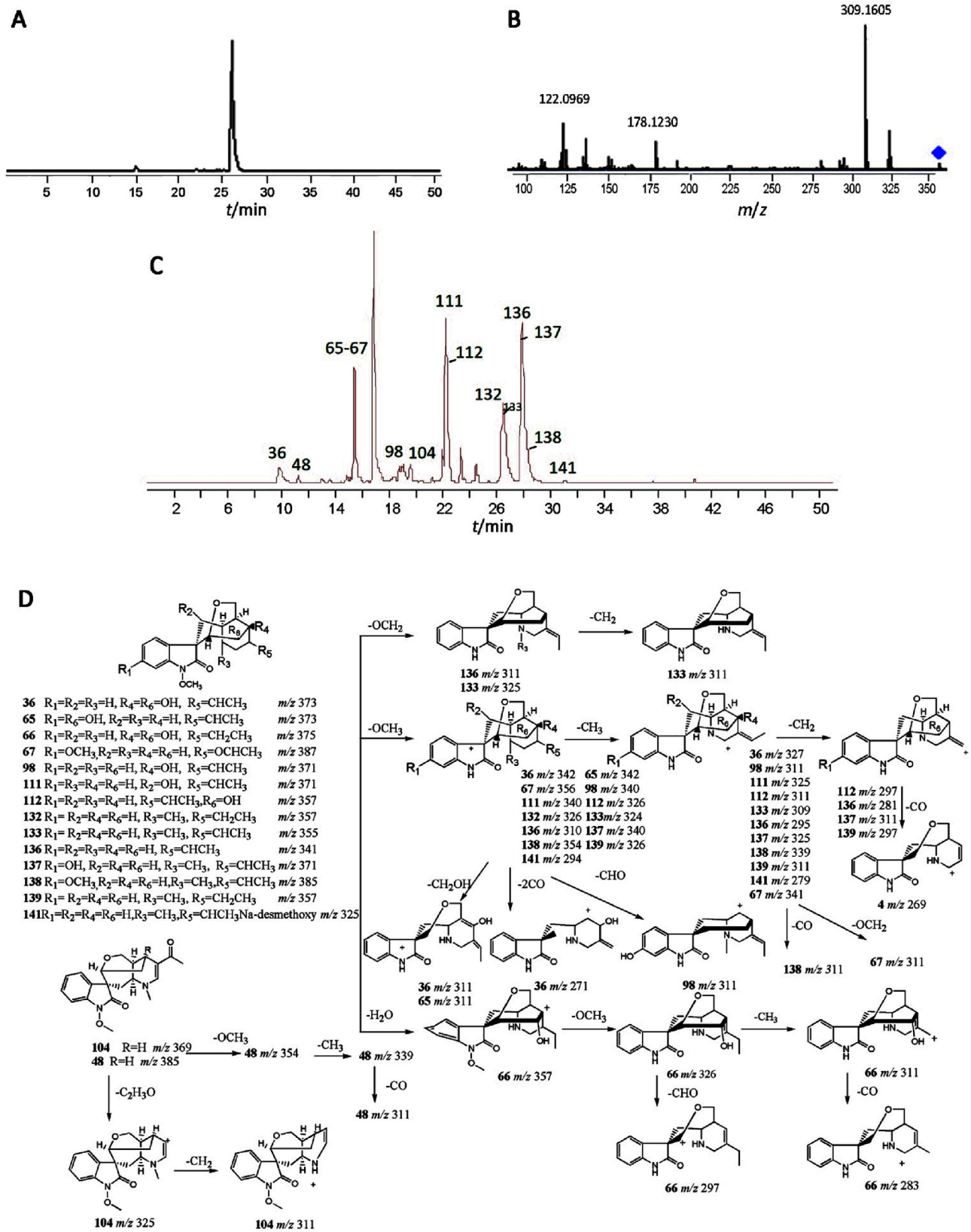

Fig. 6. EIC spectrum (A) and MS/MS spectrum (B) of component **133** (humantenine); MS/MS spectrum extracted by extracting diagnostic ions at *m*/*z* 311.17, and 311.14 (C). Mass spectral fragmentation pathways of humantenine-type alkaloids (D).

Table 2
Monitor ion pairs, CE, segment, repeatability and stability of multiple compounds in *G. elegans* samples.

No.	Analytes	t_R (min)	Ion pair	CE/ eV	Seg	Repeatability (mg/g ± RSD %)	Stability/RSD (%)
1	7-Deoxygelsemide or 9-deoxygelsemide	6.2	197.1 → 105.1	30	2	0.001 ± 3.31	3.02
2	11,14-Dihydroxygelsenicine	11.4	359.2 → 108.1	30	3	0.086 ± 2.88	1.63
3	14,15-Dihydroxygelsenicine	11.5	359.2 → 328.1	30	3	0.066 ± 2.96	2.56
4	Unknown (375)	15.6	375.2 → 311.1	30	4	0.029 ± 1.42	1.98
5	Gelsemine	16.5	323.2 → 70.1	33	4	3.787 ± 0.94	1.58
6	11-Hydroxygelsenicine	16.5	343.2 → 281.1	30	4	0.017 ± 1.27	3.42
7	Gelsemicine	17.1	359.2 → 108.1	30	4	0.002 ± 2.79	2.12
8	GSIR-1	17.4	183.1 → 91.1	30	4	0.001 ± 2.76	4.68
9	14-Hydroxygelsemicine or other hydroxylation of gelsemicine	17.5	375.2 → 313.2	35	4	0.237 ± 2.36	1.56
10	14-Hydroxygelsedine	17.8	345.2 → 285.1	30	4	0.034 ± 2.13	2.46
11	14-Hydroxygelsenicine	18.0	343.2 → 108.1	30	5	0.730 ± 3.92	1.63
12	Koumine	19.1	307.2 → 180.0	53	5	0.830 ± 1.83	2.07
13	14-Dehydroxygelsefuranidine or other dehydroxylgelsefuranidine (2)	19.4	405.2 → 343.1	30	5	0.071 ± 2.70	1.86
14	11-methoxy-14-hydroxygelsenicine	19.5	373.2 → 108.1	30	5	0.142 ± 2.16	2.69
15	Unknown (295)	19.8	295.2 → 138.1	30	5	0.058 ± 1.78	3.03
16	Hydroxyl of gelsedine	19.9	345.2 → 285.1	30	5	0.001 ± 4.46	4.20
17	Gelsemoxonine	20.1	359.2 → 311.1	30	6	0.942 ± 3.38	2.10
18	One of other 5 hit compounds	21.1	371.2 → 323.1	30	6	0.067 ± 2.84	1.64
19	14-Dehydroxygelsefuranidine or other dehydroxylgelsefuranidine (1)	21.1	405.2 → 374.2	30	6	0.049 ± 2.92	4.24
20	Koumidine	21.2	295.2 → 144.1	30	6	0.042 ± 2.01	2.06
21	14-Acetoxygelsedilam or other acetoxyl of gelsedilam (1)	21.4	373.2 → 342.2	30	6	0.005 ± 4.13	2.06
22	11-Hydroxyhumantenine	21.5	371.2 → 325.2	30	6	0.312 ± 1.77	2.26
23	Gelsevirine	22.0	353.2 → 291.2	30	7	0.191 ± 2.30	1.39
24	Gelsenicine	22.2	327.2 → 265.1	30	7	0.958 ± 1.75	1.41
25	12β-hydroxy-pregn-4,16-diene-3,20-dione	22.2	329.2 → 97.1	30	7	0.002 ± 4.96	3.00
26	Koumicine	23.8	353.2 → 166.1	30	7	0.342 ± 3.81	1.70
27	Gelsedine or Nb-Methylgelsedilam	23.4	329.2 → 298.2	30	7	0.004 ± 1.54	2.01
28	Gelseoxazolidinine	23.9	429.2 → 339.2	30	7	0.003 ± 2.53	2.99
29	16-epi-voacarpine or gelsevirine N-oxide	24.0	369.2 → 166.1	30	7	0.823 ± 1.20	1.84
30	Humantenoxenine	24.3	369.2 → 108.1	30	7	0.009 ± 3.48	3.31
31	Iso-Gelsedine or Nb-Methylgelsedilam	24.7	329.2 → 269.3	30	7	0.014 ± 4.55	2.48
32	1-O-Caffeoylquinic acid or 4-O-Caffeoylquinic acid	25.0	355.1 → 135.0	30	8	0.117 ± 1.24	1.39
33	Gelseziridine	25.7	343.2 → 108.1	30	8	0.001 ± 2.57	2.27
34	Na-Desmethoxyhumantenine	25.8	325.2 → 136.1	35	8	0.020 ± 2.63	1.55
35	14-Acetoxygelsedilam or other acetoxyl of gelsedilam (2)	26.6	373.2 → 342.2	30	8	0.033 ± 2.14	1.95
36	14-Acetoxygelsedilam or other acetoxyl of gelsedilam (3)	27.3	373.2 → 342.2	30	8	0.033 ± 2.48	2.57
37	19R-Hydroxydihydrogelsevirine or 19S-Hydroxydihydrogelsevirine	26.5	371.2 → 164.1	30	8	4.526 ± 4.24	4.18
38	11-Methoxyhumantenine	26.8	385.2 → 339.2	30	8	0.061 ± 4.33	4.53
39	*iso*-12β-Hydroxy-5α-pregn-16-ene-3,20-dione	31.2	331.2 → 109.1	30	11	0.003 ± 4.42	4.02
40	Gelse-norursane E	31.7	471.2 → 217.1	30	10	0.008 ± 4.28	3.99
41	12β-Hydroxy-5α-pregn-16-ene-3,20-dione	31.8	331.2 → 97.1	30	11	0.038 ± 4.24	4.18

compounds were higher than 0.99 in the concentration range of 10–200 ng/mL. The LODs of gelsemine, koumine, koumidine and gelsenicine were 2.5, 2, 5 and 1.5 ng/mL, respectively. The LOQs of gelsemine, koumine, koumidine and gelsenicine were 5, 5, 10 and 5 ng/mL, respectively.

The DeMRM method was examined in terms of specificity, accuracy, and stability. As presented in Fig. S4, no interfering peaks were observed at the retention times of the 41 components in the DeMRM chromatograms of *G. elegans* samples. Most componets had no the phenomenon of trailing, incomplete peak of the sample and the retention time of the sample was suitable. For example, the retention time of gelsemine was 16.5 min, and that of koumidine was 22.2 min, which indicated the specificity of this analytical method. Table 2 summarizes the relative concentrations of 41 components in the *G. elegans* sample and relative standard deviations (RSDs) of the concentrations. The intraday and interday precision were expressed as the RSD. The RSDs of the four representative components at the two tested concentrations were all within 10%. Moreover, all the RSDs of the DeMRM method were within the accepted variable limits. The results support that the DeMRM method has reasonable accuracy and stability and is applicable to the quantitative analysis of complex herbal medicines.

3.6. Sample analysis

The validated DeMRM method was subsequently applied to determine the relative concentrations of multiple components in different tissues of *G. elegans* during different periods. The quantitative performance of the DeMRM method was examined by comparing the experimental values of the four representative components obtained by DeMRM and RMRM. The DeMRM results were expressed as the relative content of herb based on a koumidine calibration curve, while the RMRM results were converted to the herb contents by calculating the absolute amounts of the components in the herb. Taking koumine in the root as an example, as shown in Fig. 7 (Root), the RMRM results indicated that the koumine content obtained from chemical standards was the highest in December, followed by September, and was the lowest in November, which is the result of RMRM. In Table 3, the relative contents of koumine obtained from the koumidine calibration curves were 1.376, 1.089, and 1.772 mg/g in September, November, and December, respectively, which indicated that the results obtained by DeMRM were consistent with the above trends observed by RMRM. The same trend proved that the results of the relative quantification of 41 components calculated by DeMRM in *G. ele-*

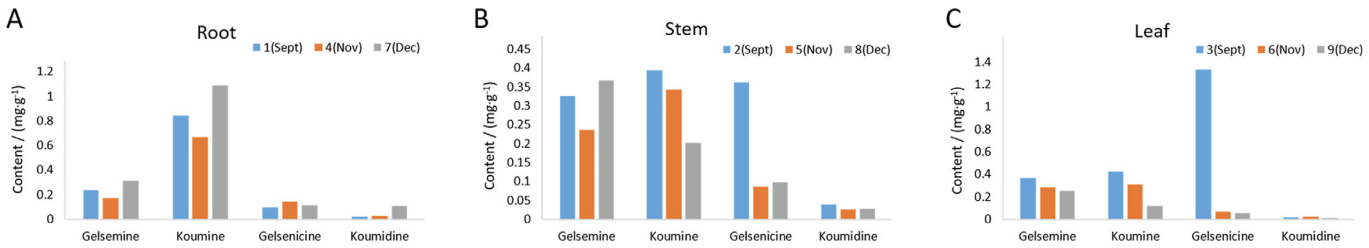

Fig. 7. Differences contents of four standards between roots (A), stems (B) and leaves (C) from *G. elegans*.

Table 3
Multi-compounds contents in *Gelsemium elegans* samples.

No.	Analytes	S1	S2	S3	S4	S5	S6	S7	S8	S9
1	7-Deoxygelsemide or 9-Deoxygelsemide	–	–	0.004	–	–	0.001	–	–	0.001
2	11,14-Dihydroxygelsenicine	0.043	0.041	0.114	0.012	0.058	0.193	0.009	0.148	0.472
3	14,15-Dihydroxygelsenicine	0.032	0.032	0.087	0.009	0.045	0.148	0.009	0.114	0.365
4	Unknown (375)	0.037	0.007	0.005	0.032	0.015	0.015	0.043	0.015	0.009
5	Gelsemine	3.036	4.145	4.679	2.208	3.014	3.565	3.956	4.678	3.19
6	11-Hydroxygelsenicine	0.048	0.032	0.08	0.008	0.039	0.009	0.002	0.003	0.006
7	Gelsemicine	–	–	–	0.001	0.001	0.002	0.003	0.004	0.004
8	GSIR-1	0.001	0.001	0.003	–	–	0.001	–	–	0.001
9	14-Hydroxygelsemicine or other hydroxylation of gelsemicine	0.424	0.145	0.129	0.273	0.187	0.13	0.417	0.136	0.088
10	14-Hydroxygelsedine	0.048	0.005	0.007	0.066	0.005	0.004	0.132	0.008	0.005
11	14-Hydroxygelsenicine	0.383	0.171	0.576	0.704	0.407	0.552	0.951	1.198	0.925
12	Koumine	1.376	0.644	0.693	1.089	0.562	0.51	1.772	0.333	0.197
13	14-Dehydroxygelsefuranidine or other dehydroxylgelsefuranidine (2)	0.076	0.037	0.106	0.064	0.041	0.143	0.117	0.03	0.097
14	11-Methoxy-14-hydroxygelsenicine	0.064	0.02	0.099	0.133	0.069	0.091	0.224	0.182	0.169
15	Unknown (295)	0.077	0.039	0.023	0.071	0.027	0.016	0.152	0.025	0.008
16	Hydroxyl of gelsedine	0.001	–	–	–	–	–	0.003	–	–
17	Gelsemoxonine	0.158	0.04	0.455	0.167	0.207	1.994	0.617	1.066	3.185
18	One of other five hit compounds	0.08	0.028	0.065	0.069	0.022	0.071	0.184	0.017	0.039
19	14-Dehydroxygelsefuranidine or other dehydroxylgelsefuranidine (1)	0.059	0.013	0.034	0.06	0.01	0.046	0.111	0.019	0.03
20	koumidine	0.022	0.04	0.02	0.028	0.028	0.022	0.107	0.028	0.012
21	14-Acetoxygelsedilam or other Acetoxyl of gelsedilam (1)	0.01	0.01	0.008	0.001	0.005	0.003	0.004	0.003	0.003
22	11-Hydroxyhumantenine	0.987	1.069	0.963	0.186	0.541	0.185	0.077	0.097	0.1
23	Gelsevirine	0.257	0.108	0.062	0.389	0.08	0.02	0.631	0.03	0.007
24	Gelsenicine	0.944	0.228	0.823	1.085	0.805	0.55	1.508	0.901	0.488
25	12β-Hydroxy-pregn-4,16-diene-3,20-dione	0.002	–	0.001	0.002	0.001	0.001	0.002	0.001	0.001
26	Koumicine	0.326	0.237	0.349	0.219	0.217	0.446	0.441	0.199	0.327
27	Gelsedine or Nb-Methylgelsedilam	0.007	0.001	0.002	0.006	0.002	0.001	0.01	0.001	0.001
28	Gelseoxazolidinine	0.015	0.005	0.01	0.002	–	0.003	0.002	–	0.001
29	16-epi-Voacarpine or gelsevirine N-oxide	0.853	0.514	0.812	0.57	0.645	1.13	0.934	0.817	1.033
30	Humantenoxenine	0.006	0.008	0.02	0.003	0.004	0.013	0.009	0.009	0.011
31	Iso-Gelsedine or Nb-Methylgelsedilam	0.012	0.002	0.002	0.042	0.001	0	0.042	0.001	–
32	1-*O*-Caffeoylquinic acid or 4-*O*-Caffeoylquinic acid	0.176	0.044	0.072	0.165	0.059	0.071	0.268	0.064	0.045
33	Gelseziridine	0.001	–	–	0.003	–	0.001	0.004	–	–
34	Na-Desmethoxyhumantenine	0.028	0.005	0.012	0.028	0.01	0.014	0.046	0.012	0.009
35	14-Acetoxygelsedilam or other Acetoxyl of gelsedilam (2)	0.039	0.008	0.019	0.068	0.019	0.02	0.069	0.019	0.019
36	14-Acetoxygelsedilam or other Acetoxyl of gelsedilam (3)	0.028	0.009	0.023	0.087	0.017	0.019	0.09	0.018	0.018
37	19R-Hydroxydihydrogelsevirine or 19S-Hydroxydihydrogelsevirine	3.436	1.261	1.335	9.918	2.4	2.677	10.567	1.584	2.629
38	11-Methoxyhumantenine	0.105	0.08	0.04	0.081	0.034	0.034	0.272	0.016	0.011
39	*iso*-12β-Hydroxy-5α-pregn-16-ene-3,20-dione	0.004	0.001	0.004	0.002	–	0.006	0.008	–	0.005
40	Gelse-norursane E	0.012	0.001	0.002	0.006	0.001	0.007	0.036	0.001	0.003

Note: -, nondetected.

gans were reliable. Although some deviation exists, the approach proposed herein still offered a direct and rapid method for semi-quantitative determination with reasonable accuracy in cases when authentic standards are not available and/or the absolute quantity is not needed.

4. Conclusion

The present work contributed to the development of a powerful integrated strategy based on liquid chromatography coupled with mass spectrometry (LC-MS) systems. The results demonstrated the significant advantages of this strategy over other strategies. First, the number of components detected with high peak intensity was successfully maximized by comprehensively optimizing the LC-QTOF/MS method, and 31 target components were characterized through matching analysis with our established personal Gelsemium database. Second, various data mining techniques, including database searching, diagnostic ion filtering and neutral loss filtering, were implemented to fully and systematically clarify the structure of various chemical components in *G. elegans*. A total of 147 components were characterized from *G. elegans*, and among them, 116 nontarget components were reported for the first time. A sensitive and reproducible LC-QqQ/MS method was successfully developed and validated for the simultaneous relative quantification of 41 components of *G. elegans*. This method was effective in identifying a variety of nontarget components and provided a tech-

nical reference for the characterization of other chemical components. The present integrated strategy would significantly contribute to chemical studies on herbal medicine, and its utility could be extended to other research fields, such as metabolomics, quality control and pharmacokinetics.

Declaration of Competing Interest

The authors declare that they have no known competing financial interests or personal relationships that could have appeared to influence the work reported in this paper.

Acknowledgments

This work was supported by National Key R&D Program of Intergovernmental Key Projects (Grant No: 2018YFE0101700) and National Natural Science Foundation of China (Grant No. 31972737).

Appendix A. Supplementary data

Supplementary data to this article can be found online at https://doi.org/10.1016/j.chmed.2020.06.002.

References

Cai, H., Xu, Q., Chang, C., Song, C., Yong, X., Yi, X., ... Jiang, H. (2014). The rapid discovery and identification of physalins in the calyx of *Physalis alkekengi* L. var. Franchetii (Mast.) Makino using ultra-high performance liquid chromatography–quadrupole time of flight tandem mass spectrometry together with a novel three-step. *Journal of Chromatography A, 1361*, 139–152.

Chen, J., Shi, Z., Song, Y., Guo, X., Zhao, M., Tu, P., & Jiang, Y. (2016). Source attribution and structure classification-assisted strategy for comprehensively profiling Chinese herbal formula: Ganmaoling granule as a case. *Journal of Chromatography A, 1464*, 102–114.

Chingin, K., Makarov, A., Denisov, E., Rebrov, O., & Zubarev, R. A. (2014). Fragmentation of Positively-Charged Biological Ions Activated with a Beam of High-Energy Cations. *Analytical Chemistry, 86*(1), 372–379.

Hao, H., Cui, N., Wang, G., Xiang, B., Liang, Y., Xu, X., Zhang, H., Yang, J., Zheng, C., Wu, L., Gong, P., & Wang, W. (2008). Global Detection and Identification of Nontarget Components from Herbal Preparations by Liquid Chromatography Hybrid Ion Trap Time-of-Flight Mass Spectrometry and a Strategy. *Analytical Chemistry, 80*(21), 8187–8194.

Hu, Y., Chen, M., Wang, Z., Lan, Y., Tang, L., Liu, M., Zhao, J., Hu, M., Zhang, L., & Ye, L. (2017). Development of a validated UPLC-MS/MS method for determination of humantenmine in rat plasma and its application in pharmacokinetics and bioavailability studies. *Biomedical Chromatography, 31*(12), e4017. https://doi.org/10.1002/bmc.v31.1210.1002/bmc.4017.

Huo, J.-H., Du, X.-W., Sun, G.-D., Dong, W.-T., & Wang, W.-M. (2018). Identification and characterization of major constituents in Juglans mandshurica using ultra performance liquid chromatography coupled with time-of-flight mass spectrometry (UPLC-ESI-Q-TOF/MS). *Chinese Journal of Natural Medicines, 16*(7), 525–545.

Jin, G.-L., Su, Y.-P., Liu, M., Xu, Y., Yang, J., Liao, K.-J., & Yu, C.-X. (2014). Medicinal plants of the genus Gelsemium (Gelsemiaceae, Gentianales)—A review of their phytochemistry, pharmacology, toxicology and traditional use. *Journal of Ethnopharmacology, 152*(1), 33–52.

Kitajima, M., Kobayashi, H., Kogure, N., & Takayama, H. (2010). New oxindole and indole alkaloids from Gelsemium rankinii. *Tetrahedron, 66*(32), 5987–5992.

Lei, X.-Q., Li, G., Cheng, L., Wang, X.-L., & Meng, F.-Y. (2018). Identification of Ligustici Rhizoma et Radix and its adulterants based on their chemical constituents by UHPLC-Q/TOF-MS combined with data mining. *Journal of Pharmaceutical and Biomedical Analysis, 154*, 123–137.

Li, W. L., Sun, X. M., Song, H., Ding, J. X., Bai, J., & Chen, Q. (2015a). Hplc/q-tof-ms-based identification of absorbed constituents and their metabolites in rat serum and urine after oral administration of cistanche deserticola extract. *Journal of Food Science, 80*(9), H2079–2087.

Li, Z., Xiao, S., Ai, N. i., Luo, K., Fan, X., & Cheng, Y. (2015b). Derivative multiple reaction monitoring and single herb calibration approach for multiple components quantification of traditional Chinese medicine analogous formulae. *Journal of Chromatography A, 1376*, 126–142.

Liang, Y., Hao, H., Kang, A. n., Xie, L., Xie, T., Zheng, X., Dai, C., Wan, L., Sheng, L., & Wang, G. (2010). Qualitative and quantitative determination of complicated herbal components by liquid chromatography hybrid ion trap time-of-flight mass spectrometry and a relative exposure approach to herbal pharmacokinetics independent of standards. *Journal of Chromatography A, 1217*(30), 4971–4979.

Ling, Q., Liu, M., Wu, M.-X., Xu, Y., Yang, J., Huang, H.-H., & Yu, C.-X. (2014). Anti-allodynic and Neuroprotective Effects of Koumine, a Benth Alkaloid, in a Rat Model of Diabetic Neuropathy. *Biological|Pharmaceutical Bulletin, 37*(5), 858–864.

Liu, M., Huang, H.-H., Yang, J., Su, Y.-P., Lin, H.-W., Lin, L.-Q., Liao, W.-J., & Yu, C.-X. (2013). The active alkaloids of *Gelsemium elegans* Benth. are potent anxiolytics. *Psychopharmacology (Berl), 225*(4), 839–851.

Liu, Y.-C., Lin, L. i., Cheng, P. i., Sun, Z.-L., Wu, Y., & Liu, Z.-Y. (2017a). Fingerprint analysis of *Gelsemium elegans* by HPLC followed by the targeted identification of chemical constituents using HPLC coupled with quadrupole-time-of-flight mass spectrometry. *Fitoterapia, 121*, 94–105.

Liu, Y.-C., Xiao, S. a., Yang, K., Ling, L. i., Sun, Z.-L., & Liu, Z.-Y. (2017b). Comprehensive identification and structural characterization of target components from *Gelsemium elegans* by high-performance liquid chromatography coupled with quadrupole time-of-flight mass spectrometry based on accurate mass databases combined with MS/M: Structural characterization of Gelsemium elegans components by LC-QqTOF MS. *J. Mass Spectrom., 52*(6), 378–396.

Ma, X.-D., Fan, Y.-X., Jin, C.-C., Wang, F., Xin, G.-Z., Li, P., & Li, H.-J. (2016). Specific targeted quantification combined with non-targeted metabolite profiling for quality evaluation of *Gastrodia elata* tubers from different geographical origins and cultivars. *Journal of Chromatography A, 1450*, 53–63.

Meyer, L., Boujedaini, N., Patte-Mensah, C., & Mensah-Nyagan, A. G. (2013). Pharmacological effect of gelsemine on anxiety-like behavior in rat. *Behavioural Brain Research, 253*, 90–94.

Mustafa, A. M., Eldahmy, S. I., Caprioli, G., Bramucci, M., Quassinti, L., Lupidi, G., Beghelli, D., Vittori, S., & Maggi, F. (2018). Chemical composition and biological activities of the essential oil from *Pulicaria undulata* (L.) C. A. Mey. Growing wild in Egypt. *Natural Product Research*, 1–5.

Ornduff, R. (1970). The systemetics and breeding system of *Gelsemium* (Loganiaceae). *Journal of the Arnold Arboretum, 51*(1), 1–17.

Qiao, X., Li, R. u., Song, W., Miao, W.-J., Liu, J., Chen, H.-B., Guo, D.-a., & Ye, M. (2016). A targeted strategy to analyze untargeted mass spectral data: Rapid chemical profiling of *Scutellaria baicalensis* using ultra-high performance liquid chromatography coupled with hybrid quadrupole orbitrap mass spectrometry and key ion filtering. *Journal of Chromatography A, 1441*, 83–95.

Samanipour, S., Reid, M. J., Bæk, K., & Thomas, K. V. (2018). Combining a Deconvolution and a Universal Library Search Algorithm for the Nontarget Analysis of Data-Independent Acquisition Mode Liquid Chromatography−High-Resolution Mass Spectrometry Results. *Environmental Science and Technology, 52*(8), 4694–4701.

Shi, X. J., Yang, W. Z., Qiu, S., Yao, C. L., Shen, Y., Pan, H. Q., ... Guo, D. A. (2017). An in-source multiple collision-neutral loss filtering based nontargeted metabolomics approach for the comprehensive analysis of malonyl-ginsenosides from *Panax ginseng*, p.Quinquefolius, and p.Notoginseng. *Analytica Chimica Acta, 952*, 59–70.

Shi, W., Zhang, C., Zhao, D., Wang, L., Li, P., & Li, H. (2018). Discovery of Hepatotoxic Equivalent Combinatorial Markers from Dioscorea bulbifera tuber by Fingerprint-Toxicity Relationship Modeling. *Scientific Reports, 8*(1). https://doi.org/10.1038/s41598-017-18929-z.

Tan, J., Zheng, M., Duan, S., Zeng, Y., Zhang, Z., Cui, Q., Zhang, J., Hong, T., Bai, J., & Du, S. (2018). Chemical profiling and screening of the marker components in the fruit of *Cassia fistula* by hplc and uhplc/ltq-orbitrap ms(n) with chemometrics. *Molecules, 23*(7), 1501–1507.

Wang, H., Shi, S., & Wang, S. (2018). Can highly cited herbs in ancient Traditional Chinese medicine formulas and modern publications predict therapeutic targets for diabetes mellitus?. *Journal of Ethnopharmacology, 213*, 101–110.

Wang, L., Wen, Y., & Meng, F. (2018). Simultaneous determination of gelsemine and koumine in rat plasma by UPLC-MS/MS and application to pharmacokinetic study after oral administration of *Gelsemium elegans* Benth extract. *Biomedical Chromatography, 32*(6), e4201. https://doi.org/10.1002/bmc.v32.610.1002/bmc.4201.

Xiao, S. a., Huang, Y.-J., Sun, Z.-L., & Liu, Z.-Y. (2017). Structural elucidation of koumine metabolites by accurate mass measurements using high-performance liquid chromatography/quadrupole-time-of-flight mass spectrometry: Structural elucidation of koumine metabolites by HPLC/QqTOF-MS. *Rapid Communications in Mass Spectrometry, 31*(3), 309–314.

Xu, Y., Qiu, H. Q., Liu, H., Liu, M., Huang, Z. Y., Yang, J., & Yu, C. X. (2012a). Effects of koumine, an alkaloid of gelsemium elegans benth., on inflammatory and neuropathic pain models and possible mechanism with allopregnanolone. *Pharmacology Biochemistry and Behavior, 101*(3), 504–514.

Xu, Y.-K., Liao, S.-G., Na, Z., Hu, H.-B., Li, Y., & Luo, H.-R. (2012b). Gelsemium alkaloids, immunosuppressive agents from *Gelsemium elegans*. *Fitoterapia, 83*(6), 1120–1124.

Yamada, Y., Kitajima, M., Kogure, N., Wongseripipatana, S., & Takayama, H. (2011). Seven new monoterpenoid indole alkaloids from *Gelsemium elegans*. *Chemistry - An Asian Journal, 6*(1), 166–173.

Yan, Y., Chai, C.-Z., Wang, D.-W., Yue, X.-Y., Zhu, D.-N., & Yu, B.-Y. (2013). HPLC-DAD-Q-TOF-MS/MS analysis and HPLC quantitation of chemical constituents in traditional Chinese medicinal formula Ge-Gen Decoction. *Journal of Pharmaceutical and Biomedical Analysis, 80*, 192–202.

Yang, K., Huang, Y.-J., Xiao, S. a., Liu, Y.-C., Sun, Z.-L., Liu, Y.-S., & Liu, Z.-Y. (2018a). Identification of gelsemine metabolites in rat liver S9 by high-performance liquid chromatography/quadrupole-time-of-flight mass spectrometry. *Rapid Communications in Mass Spectrometry, 32*(1), 19–22.

Yang, K., Long, X.-M., Liu, Y.-C., Chen, F.-H., Liu, X.-F., Sun, Z.-L., & Liu, Z.-Y. (2018b). Development and in-house validation of a sensitive LC–MS/MS method for

simultaneous quantification of gelsemine, koumine and humantenmine in porcine plasma. *Journal of Chromatography B, 1076*, 54–60.

Yang, Y., Wang, H.-J., Yang, J., Brantner, A. H., Lower-Nedza, A. D., Si, N., Song, J.-F., Bai, B., Zhao, H.-Y., & Bian, B.-L. (2013). Chemical profiling and quantification of Chinese medicinal formula Huang-Lian-Jie-Du decoction, a systematic quality control strategy using ultra high performance liquid chromatography combined with hybrid quadrupole-orbitrap and triple quadrupole mass spectrometers. *Journal of Chromatography A, 1321*, 88–99.

Zhang, X., Chen, Y. i., Gao, B. o., Luo, D., Wen, Y., & Ma, X. (2015a). Apoptotic Effect of Koumine on Human Breast Cancer Cells and the Mechanism Involved. *Cell Biochemistry and Biophysics, 72*(2), 411–416.

Zhang, J. Y., Wang, Z. J., Li, Y., Liu, Y., Cai, W., Li, C., ... Qiao, Y. J. (2016). A strategy for comprehensive identification of sequential constituents using ultra-high-performance liquid chromatography coupled with linear ion trap-orbitrap mass spectrometer, application study on chlorogenic acids in flos *Lonicerae japonica*. *Talanta, 147*(62), 16–27.

Zhang, S., Hu, S., Yang, X., Shen, J., Zheng, X., Huang, K., & Xiang, Z. (2015b). Development of a liquid chromatography with mass spectrometry method for the determination of gelsemine in rat plasma and tissue: Application to a pharmacokinetic and tissue distribution study: Liquid Chromatography. *Journal of Separation Science, 38*(6), 936–942.

Zhang, W., Zhang, S.-Y., Wang, G.-Y., Li, N.-P., Chen, M.-F., Gu, J.-H., & Ye, W.-C. (2017a). Five new koumine-type alkaloids from the roots of *Gelsemium elegans*. *Fitoterapia, 118*, 112–117.

Zhang, Y. u., Cheng, Y., Liu, Z., Ding, L., Qiu, T., Chai, L., & Chen, X. (2017b). Systematic screening and characterization of multiple constituents in Guizhi Fuling capsule and metabolic profiling of bioactive components in rats using ultra-high-performance liquid chromatography/quadrupole-time-of-flight mass spectrometry. *Journal of Chromatography B, 1061-1062*, 474–486.

Zuo, M.-T., Liu, S.-S., Lin, L., Wang, Z.-Y., Bai, X., Sun, Z.-L., & Liu, Z.-Y. (2018). Characterization of *N* -methylcanadine and *N* -methylstylopine metabolites in rat liver S9 by high-performance liquid chromatography/quadrupole time-of-flight mass spectrometry. *Rapid Communications in Mass Spectrometry, 32*(23), 2047–2054.